"Comparison of Flow Models at Different Scales Using the 10th SPE Comparative Solution Project"

A THESIS IN PARTIAL FULFILLMENT OF THE REQUIREMENTS FOR THE DEGREE OF

"MASTER OF SCIENCE"

SUBMITTED TO THE "NATURAL RESOURCES AND PETROLEUM ENGINEERING" DEPARTMENT

MONTANUNIVERSITÄT LEOBEN, AUSTRIA

Written by

Magdi Asadig Abunaja, BSc

Under supervision of

Univ.Prof. Dipl.-Ing. Dr.mont. Leonhard Ganzer

October 2007

Acknowledgments

First of all, I would like to thank God, the Almighty, for having made everything possible by giving me strength and courage to do this work.

My deepest gratitude to Prof. Dr. Leonhard GANZER, my supervisor, for his unselfishness, encouragement and guidance and patience he demonstrated during my study.

Sincere thanks to my family, and friends who all gave me courage and support.

Table of Contents

List of Figures

List of Tables

Kurzfassung

Um die Effekte, die durch Heterogenität der Gesteine ausgelöst werden, in der Lagerstättensimulation zu berücksichtigen, müssen diese auf alle Gittergrössen richtig angepasst werden. Das Werkzeug, das zu dieser Transformation von Informationen von kleinen zu grösseren Gitterblöcken benutzt wird, sind die Upscaling Methoden. Diese Algorithmen weisen den Gitterzellen passende Werte für Porosität, Permeabilität oder anderen Eigenschaften zu.

Diese Diplomarbeit beschäftigt sich mit Verhalten von Simulationsmodellen verschiedener Grösse und Auflösung, die alle vom selben, hochauflösenden geologischen Modell stammen. Die verschiedenen Modellgrössen wurden mithilfe von Upscaling Methoden erzeugt.

Die erste angewandte Methode ist die analytische Methode, bei der die Eigenschaften durch algebraische Gleichungen berechnet wurden.

Die zweite Methode ist eine numerische mit dem Namen ‚Diagonal Tensor' Methode, bei der die Permeabilität mithilfe von numerischer Simulation den grösseren Gitterblöcken zugeordnet wird.

Als Referenzmodell wurde das 10. SPE Vergleichsmodell in allen Fällen verwendet, um die Upgridding und Upscaling Lösungen und auch deren dynamisches Fliessverhalten zu vergleichen.

Das Originalmodell hat mehr als eine Million Gitterblöcke. Allerdings sind die Laufzeiten der kleineren Modelle in der Praxis wünschenswerter.

Die Petrel Software wurde in dieser Studie zum Upscaling verwendet. Eclipse 100 war der Lagerstättensimulator, mit dem alle Simulationen durchgeführt wurden.

Abstract

In order to retain the effect of heterogeneities at all scales in the fluid flow simulation, available data on fine scale must be transferred to coarser scales. The tools used for this transformation are the upscaling algorithms, which assign suitable values of porosity, permeability, and other flow functions to cells on the coarse simulation grid.

This master thesis describes the behavior of different flow models at various scales all derived from the same fine-scale geological model. The different flow models were generated using upscaling methods.

The first upscaling approach used is the analytical method where the properties were upscaled by algebraic equations.

The second upscaling method is numerical method, the diagonal tensor method was used specifically to upscale permeability from a fine geological grid to a coarser simulation grid.

The 10th SPE Comparative Solution Project was used in all cases to compare upgridding and upscaling approaches and the ability to compare performance of a waterflood.

The original model has a simple geometry with more than one-million cells. It would be hard, though not impossible, to simulate the fine grid model in a reasonable time using conventional fine difference (FD) simulation techniques.

Petrel^{TM} software was used in this work to perform the upscaling. Eclipse 100 software was used to perform the dynamic flow simulation of the models at different scales.

Chapter 1

1 Technical Description of the Upscaling Problem.

1.1 Introduction

Through advanced reservoir characterization techniques, it is common to model the geologic structure and stratigraphy of a reservoir with millions of grid cells, each cell populated with a reservoir property that includes, but is not limited to, rock type, porosity, permeability, initial interstitial fluid saturation, and relative permeability and capillary pressure functions. However, reservoir simulations are typically performed with far fewer grid cells. The direct use of fine-grid models for reservoir simulation is not generally feasible because their fine level of detail places prohibitive demands on computational resources. Therefore, a method is needed to transform or to scale up the fine-grid geologic reservoir model to a coarse-grid simulation model while preserving, as much as possible, the fluid flow characteristics of the fine-grid model.

One key fluid flow property for reservoir simulation is permeability. Permeability is the ability of a rock to transmit fluids through interconnected pores in the rock. It can vary substantially within a hydrocarbon-bearing reservoir. Typically, permeabilities are generated for fine-scale models (geologic models) using data from well core samples. For simulation cells, the heterogeneities of the geologic model are accounted for by determining an effective permeability. An effective permeability of a heterogeneous medium is typically defined as the permeability of an equivalent homogeneous medium that, for the same boundary conditions, would give the same flux (amount of fluid flow across a given area per unit time). Determining an effective permeability, commonly called permeability upscaling, is not straightforward. The main difficulty lies in the interdependent influences of permeability heterogeneities in the reservoir and the applied boundary conditions.

Many different upscaling techniques have been proposed. Most of these techniques can be characterized as (1) direct methods or (2) flow-based methods. Examples of direct methods are simple averaging of various kinds (e.g., arithmetic, geometric and harmonic averaging) and successive renormalization[1]. Flow-based upscaling is a more sophisticated method designed specifically for permeability. It involves performing a flow simulation on the block of fine cells coinciding with each coarse cell to determine a representative coarse cell permeability value. The tensor upscaling process will calculate I, J, and K or X, Y, and Z permeabilities from input as permeability in the I, J and K directions, net-to-gross and porosity[2].

The term upscaling is used in the literature to describe two process: (1) upgridding, whereby the fine grid is coarsened in such a way to preserve the fractional flow as well as the breakthrough characteristics of the fine grid and (2) actual upscaling, where by the properties of the fine grids are analytically or numerically converted to estimate effective properties for the coarsened grid[3].

Once the fine model is optimally coarsened, the next step is to calculate the effective properties by upscaling. There are two types of properties: (1) scalar properties such as porosity that is averaged arithmetically with volume or pore volume weighting and (2) tensorial properties, specifically permeability, which can be upscaled in many ways. The pressure solver algorithm is used to upscale single phase fluid flow systems. This approach requires specific boundary conditions to calculate effective permeabilties that honor the fine-grid performance and can be incorporated directly into the -simulator[4].

1.2 Data Flow in Conventional Simulation

A geological reservoir model should be the result of incorporating all information that is available. In addition to the data available from the reservoir itself, like well data, seismic and production data, the geologist will also use geological studies from fields in the area (if there are any). He or she would make a basin wide interpretation of the depositional systems. To understand these better, modern depositional analogs and outcrop information is used to increase the understanding on how the rocks in this reservoir were deposited and how tectonics and diagenesis may have altered the reservoir after burial.

Any reservoir model is only one realization of a large number of possible models for this reservoir. All reservoir modelling contains uncertainties - A model is never the model of the reservoir, but should express our best possible understanding of the reservoir. To get more accurate estimations of hydrocarbon volumes and flow properties of a reservoir, uncertainty analysis should be performed, incorporating uncertainties of our interpretation, depth conversion, modelling, facies modelling, petrophysical modelling etc. (Figure 1-1) shows the typical data flow.
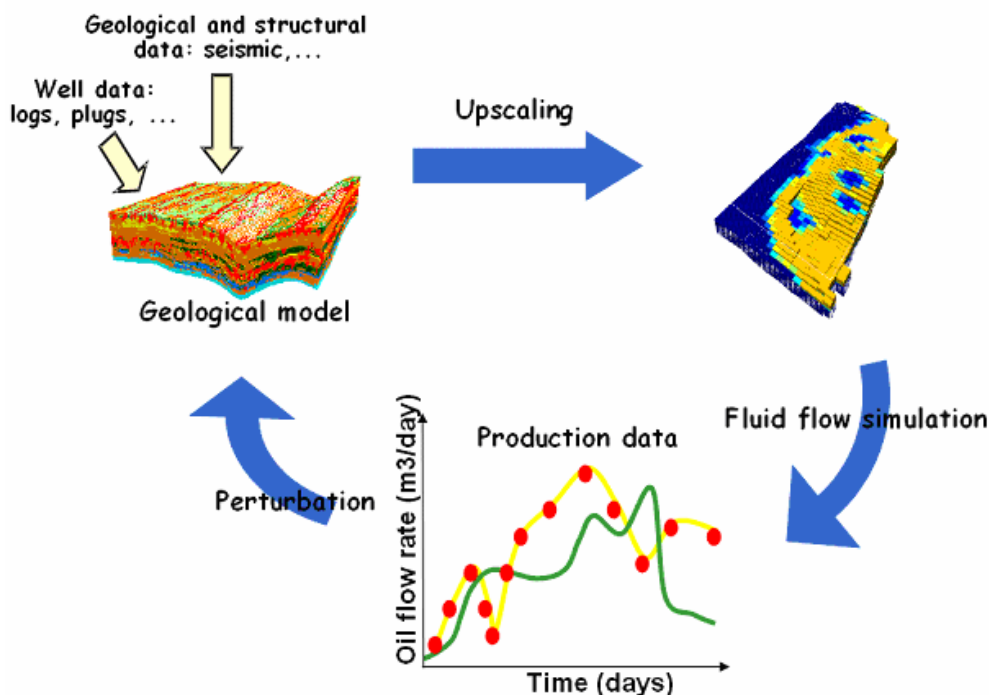
Figure (1-1): Data flow in conventional simulation

1.2.1 Building the Structure Model

Building the reservoir structure model refers to the combined work of defining the structural top map of the hydrocarbon accumulation and interpreting the fault pattern those effects the reservoir.

Traditionally, this phase of the study is the domain of geophysics. Seismic surveys actually offer the only direct means to visualize the subsurface structures and to infer a geometrical model for the reservoir. While other techniques can provide useful information about the structures setting of the reservoir under study, e.g., regional tectonic studies, there is little doubt reservoir geophysics, either 2D or 3D, still represents in practically all cases the reference source of large scale information [5].

1.2.2 Building the Property Model

One of the principal tasks of the petroleum geologist is the zoning of well logs or core data into geological units. These units are correlated and inter- or extrapolated across the field in order to obtain genetic units that serve as building blocks of the geological model of the field. Once a representation of the petrophysical properties for the layers has been obtained, a three-dimensional property model can be constructed. The fine-scale property model will be upscaled, or lumped into larger units that become the building blocks for the reservoir model used in reservoir simulation [6].

1.2.3 Building a Simulation Model from Geological Model

A successful reservoir simulation requires detailed knowledge of geological models. The First step is the upgridding whereby the size and location of the simulation blocks as a function of spatial position are designed. Vertically the block size is decided by lumping the fine layers into coarse layers. Areally, rows and columns of geological cells can be grouped. The second stage is upscaling of the data. After successfully building the coarse scale blocks, properties are then assigned to them [7].

1.3 Classification of Upscaling Methods

Research has been on going to find and to develop a new algorithm that gives the best representation for calculating the effective properties of the fluid flow. Several of these algorithms are publicly and commercially available for upscaling by using either analytical or numerical approaches and even generating pseudo functions (pseudo relative permeability and capillary pressure) based on the reservoir simulation of the fine grid model. Simple method, such as arithmetic, geometric and harmonic averages to the more complicated tensor methods, such as diagonal tensor and full tensor methods have been developed and exist commercially.

Each individual algorithm's function, advantages and disadvantages will be capture in this section.

1.3.1 Analytical Methods

1.3.1.1 Arithmetic, Geometric and Harmonic Averages

The analytical methods such as arithmetic, geometric and harmonic averages have been regarded as the fastest and intuitively simple methods for upscaling. Earlier research by Warren and Price in 1961 and Bower in 1969 indicated that the effective permeability behaved geometrically based on Monte Carlo simulation and analog simulation in 2D flow field respectively. Further analysis by Freeze in 1975 indicated that the harmonic mean is representative of the homogeneous conductivity based on the steady state and 1D transient ground water flow in non-uniform media.

The arithmetic, harmonic and geometric averages can be expressed as shown in the Equation (1-1), Equation (1-2) and Equation (1-3) respectively.

$$\overline{k}_{x.A} = \frac{1}{n}\sum k_{xi,j.k} \qquad (1\text{-}1)$$

Arithmetic Average

$$\overline{k}_{x.H} = \frac{n}{\sum\limits_{i.j.k} K^{-1}_{xi.j.k}} \qquad (1\text{-}2)$$

Harmonic Average

$$\overline{k}_{x.G} = \left[\Pi_{i,j,k} k_{xi,j,k} \right]^{1/n} \qquad (1\text{-}3)$$

Geometric Average

Some of these methods (e.g. harmonic and geometric methods), however, would be disadvantageous if there was a nil value present in the fine scale system, which is sometimes defined as non-flow or barrier in the system (shale or undefined/non-active cells in the system). With any nil value present in the system, the effective permeability would create an undefined heterogeneity of the reservoir. Thus, it is resulting in a limited range for validity. Furthermore, any undefined heterogeneity of the reservoir needs to be reported, such that a treatment in barrier preventing any vertical communication through it and a vertical permeability (Kv) determination for blocking the wells can be treated appropriately.

In addition to these nil value limitations, these methods can only solve a single direction of the effective permeability for determining the effective permeability. This is not the case in real life, as permeability is a directional property of fluid flow in porous media. Furthermore, it suffers from some limitations in applicability.

Most reservoirs are generally more laterally homogeneous compared to their vertical direction. Therefore, due to the reservoir's heterogeneity nature, arithmetic average, as it derived based on parallel sequences of layered reservoir beds, is believed to represent upper bound of the effective permeability value. On the other hand, on the vertical direction of the reservoir bedding, it is derived based on serial sequences of beds or perpendicular to the bedding, is believed represent the lower bound of the effective permeability values by taking in to consideration the lowest permeability as the dominant ones. Derivations of these algorithms are summarized in Appendix A.

According to Dagan 1979, this theory holds true, as the effective permeability is between the arithmetic and harmonic mean of the heterogeneous reservoir. Furthermore, Dagan (1982) also states that under unsteady state, the effective hydraulic conductivity is time dependent and shows a deviation from arithmetic means at an early time. Thus, the reservoir will first flow laterally compared to its vertical direction as they are behaving more homogeneously and more connected compared to the vertical flow.

The geometric average algorithm is also believed to take into consideration both harmonic and arithmetic effects of the effective permeability (i.e. the mid point between the upper and lower bound of the effective permeability values). It is a good estimator for lognormal isotropic fine scale permeability when the range is smaller than the size of the coarse scale block. Also, when the permeability is distributed randomly to flow direction, that is, in a heterogeneous, unstructured reservoir, this geometric average will be a good estimator. Thus, it is often used conventionally as the effective permeability value for numerical simulations.

The above statement concurs with Smith and Freez's (1979) findings. They stated that the geometric mean would accurately predict the average behavior of hydraulic conductivity, which statistically would behave homogeneously with isotropic covariance function. However, in 2D and 3D, this simple algorithm can become less accurate as the effective conductivity is a function of spatial distribution and system dimensionality. Furthermore, this tends to influence the lower permeabilities in many reservoirs and disregard the potentially significant high permeability streaks, which will be the main preferential path in the reservoir. The selection of these mentioned algorithms is normally based on the rock fabric and fluid flow direction. However, this is only realistic if certain conditions are met, such as single-phase fluid in homogeneous, or simple heterogeneous, reservoir with continues layers. For example reservoirs, these algorithms are no longer valid and upscaling with numerical simulations will be required which involves running the fine grid simulation to calculate the effective permeability at a coarser scale.

1.3.1.2 **Power Average**

Another analytical algorithm that can be used is the power average. It is a fast and simple intuitive method similar to any other analytical algorithm. Journel et al. (1986) based his experiment on the indicator approach to generate realization of sand shale proportion in the system. He generated the permeability field, which was highly variable, highly anisotropy and whose spatial distribution and correlation covered multiple scales of variability. It was found that the effective permeability, based on Monte Carlo simulation for various shall/sand proportions, could be fitted using the power average model.

The equation for power average is shown below in Equation (1-4)

$$k_{x,p,\omega} = \left[\frac{1}{n} \sum_{i,j,k} k_{xi,j,k}^{\omega} \right]^{\frac{1}{\omega}}$$

(1-4)

Power Average

The power average model requires the power factor, which should be in the range of between -1 and 1. The power factor of -1 (ω=-1) basically represents the harmonic average, while the power factor of 1 (ω=1) represent the arithmetic mean. The power factor of 0 (ω=-0) represent the geometric mean of the heterogeneous system. It was also found that a power factor of 0.57 (ω=0.57) is the best-characterized horizontal flow in shale-sand environments, and a power factor of 0.12 is the best characterized for vertical flow.

The drawback of the power average is similar to the rest of the analytical methods, which are limited to solving only 1D direction and also misleading with the presence of nil values for power factor less than 0. This factor, however, is quite sensitive to such factors as the shale geometry, dimensions of blocks relative to correlation range and it's nature to multi model distribution.

Gomez-Hernandez and Gorelick in 1989 found that the effective hydraulic conductivity could be determined based on power average models using exponents

between harmonic and geometric mean distribution. They based their research on the investigation of spatial variability of aquifer hydraulic conductivity influences on hydraulic head, under steady state flow for stochastic approach with conditional and unconditional simulation. They also stated that the effective hydraulic conductivity is a function of distribution type, anisotropy, correlation length and boundary conditions.

Furthermore, the power exponent is often calculated to replicate the performance of the more computing extensive fluid flow based methods and to determine a proper chosen exponent. In this way, it becomes particularly useful and less time consuming for upscaling a large number of realizations of a reservoir.

1.3.1.3 Renormalization

Renormalization generally means the procedure for redefining fundamental process into larger scales. The renormalization procedure was developed originally for the purpose of removing divergences in quantum field theory. A huge body of literature on renormalization exists in quantum field theory, statistical physics, and other fields. Early application of the renormalization procedure is flow in porous media include King (1989), who used this technique for upscaling permeability values on numerical grids. As illustrated in figure (1-2), the permeability value at the two-dimensional, fine grid of 2^6 (or , more generally, 2^{Nd}, where d is the space dimensionality) meshes are processed to obtain the rescaled (or renormalized) values at the coarser one with 2^4 (or, $2^{(N-1)d}$) meshes. This procedure id repeated until a grid of the desired size is reached. It is seen that renormalization is recursive algorithm. The permeability values at the finer grid are implicitly accounted for through the renormalized values at the coarse grid. However, there is no universal theoretical formula in two and three dimensions for calculating the renormalized values at the coarse grid. However, there is no universal theoretical formula in two and three dimensions for calculating the renormalized (upscaled, block, or equivalent) permeabilities values at the finer scales. In the two dimensional case, the renormalized permeability at each block needs to be calculated from the four sub-blocks at the finer level. This calculation can be done either numerically or analytically. A numerical approach for calculating the renormalized (block) permeability values can be computationally very expensive if a

large number of blocks are involved [9].
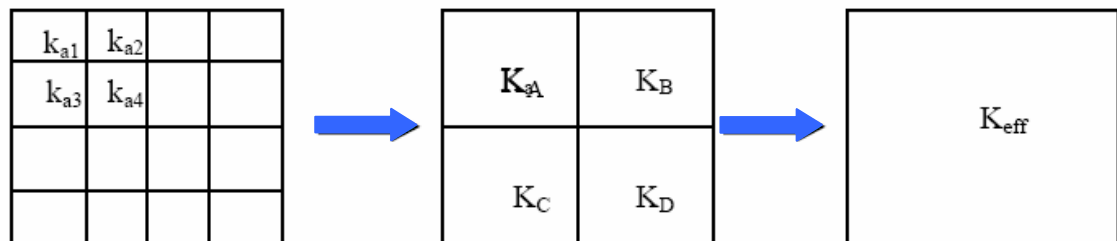
Figure (1-2): illustration of the renormalization procedure.

1.3.2 Numerical Methods

Numerical techniques are the other available upscaling tool. A myriad of numerical methods has been proposed by different researchers [9, 10]. Most of these methods are capable of providing higher accuracy than the analytical procedures; however, they require a sectorial solution of the flow equation at the fine scale, which is time consuming. Numerical upscaling is normally used for local or cross sectional modeling in situations where maximum accuracy is desirable [10].

1.3.2.1 Diagonal Tensor Based on Periodic Boundary Conditions

The diagonal tensor algorithm is basically based on Darcy's law fluid flow equation and the law of mass conservation. The following diagram in Figure (1-4) is the basic principle of the diagonal tensor algorithm.

The geometry of the fine scale cells is firstly calculated and determined in the calculation. The appropriate pressure drop and the boundary conditions in the specific directions are then applied and calculated to determine the effective properties. This basically applies some pressure on the inlet to force the fluid flow from left to right in the x direction, while assuming that there is no flow across to the other directions, as shown below as a solid line. The boundary condition is specified to be at a constant

pressure of one at the inlet stream and a constant pressure of 0 at the outlet stream, shown in Figure (1-3).

$$\frac{\partial p}{\partial y} = 0$$

$p_1 = 1$ $p_2 = 0$

$$\frac{\partial p}{\partial y} = 0$$
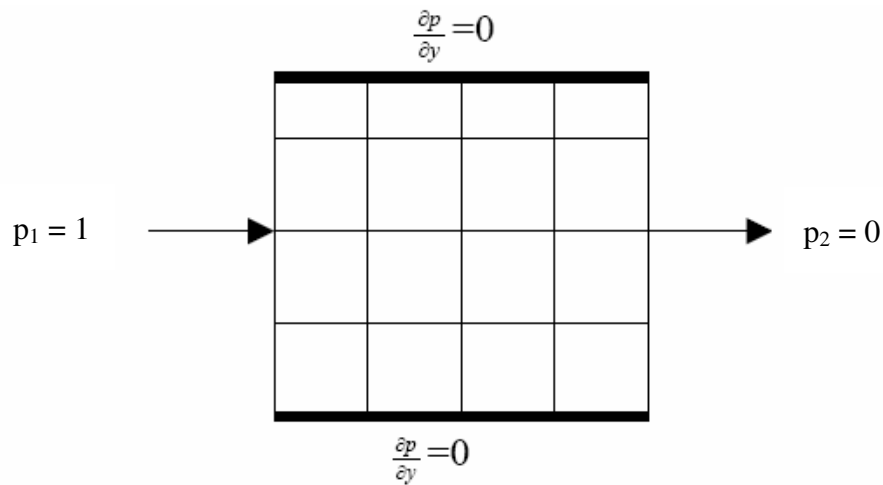
Figure (1-3) pressure and boundary condition assumptions for diagonal tensor

The pressure in each fine scale grid inside the coarse grid block and the mass flux across the system are solved by applying appropriate Darcy's law fluid flow equation (1-5) as shown below:

$$q = \frac{k.A}{\mu} \frac{\left(p_1 - p_2\right)}{L} \qquad \text{(1-5)}$$

Darcy's law of fluid flow equation
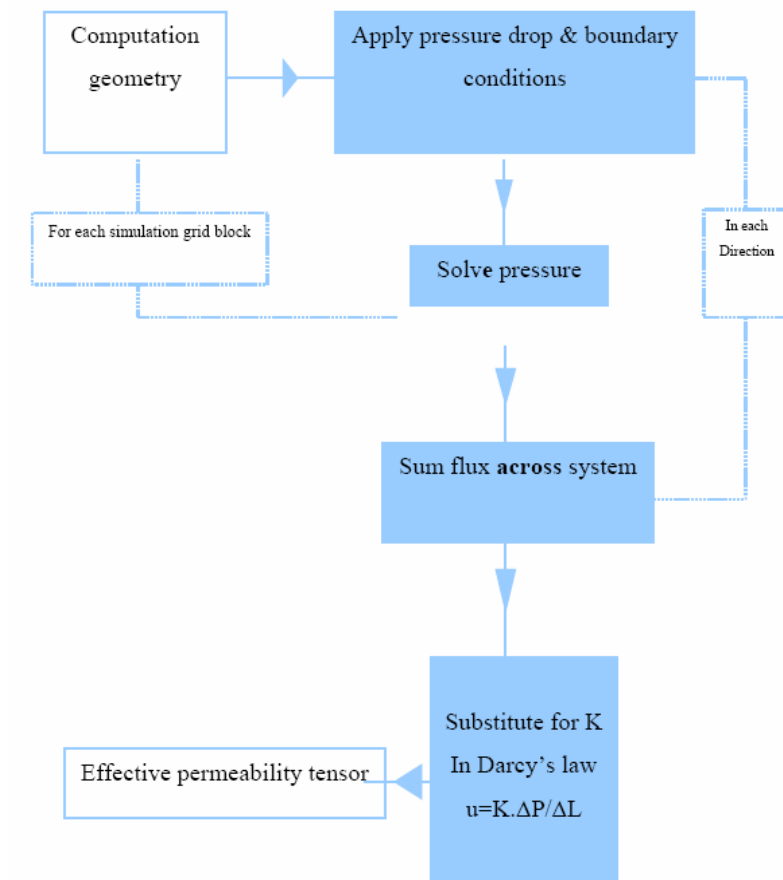
Figure (1-4) process flowchart on how diagonal tensor is derived

In reality there should not be a change in flux between the fine grid system and the single coarse grid system. Hence, the flux across the system is then assumed up to obtain the single value flux at the coarse grid.

By using Darcy's equation again, the effective permeability can then be obtained in equation (1-6).

$$k_{eff} = q_{finescale} \, \Delta x / A \qquad\qquad\qquad (1\text{-}6)$$

Effective permeability by rearranging the Darcy's law equation

The above procedures are then repeated to obtain the diagonal tensor permeability (k_{xx}, k_{yy}, k_{zz}) by applying a periodic boundary to the appropriate directions [8].

1.3.2.2 Full Tensor Based on Periodic Boundary Conditions

In subsurface flow, Darcy's law is used to describe fluid flux. The permeability tensor k in three-dimensional space is given by:

$$k = \begin{bmatrix} k_{xx} & k_{xy} & k_{xz} \\ k_{xy} & k_{yy} & k_{yz} \\ k_{xz} & k_{yz} & k_{zz} \end{bmatrix}$$

If the directions of eigenvectors of k are aligned with the axes of the coordinate system then k is a diagonal tensor given by:

$$k = \begin{bmatrix} k_{xx} & & \\ & k_{yy} & \\ & & k_{zz} \end{bmatrix}$$

In general, the principal directions of the permeability tensor are not aligned with the axes of the coordinate system in which the flow equations are solved. This is especially true for geometrically complex strata. The result of this offset between the two coordinate systems is the requirement to use full tensor permeabilities. However, most current simulators do not have the capability to model this type of permeability. Advances in reservoir characterization and geostatistics have facilitated the construction of fine scale reservoir images. Some degree of upscaling is almost always required to make the problem computationally amenable. The upscaled permeabilities calculated thus are, in general, full tensor quantities. Finite difference formulations using a nine-point computational molecule were independently developed. In this type of approach, grid orientation effect was reduced and full tensor permeability was incorporated. However, it was still difficult to represent highly complex geometry using this approach [11].

1.3.3 Pseudo Methods

There are also several multiphase upscaling algorithms, which have been used widely for reservoir upscaling. It is relatively complicated to compare the pseudo methods to the single-phase upscaling as it involves a complex solution between rock properties and fluid flow effects. There are two categories for pseudo methods, which are static and dynamic pseudo methods. Each method will be discussed in detail.

1.3.3.1 Static Pseudo Method

The static pseudo method is the simplest form of the pseudo methods. Pseudo properties are generated for inputs to the reservoir simulation and dynamic impacts such as the variability of pressure with respect to time and other properties are ignored in this method. The most widely used static pseudo methods are probably the Coast, Hearn, Stiles and Dykstra/Parson methods [8].

Prior to use of any of the above mentioned static pseudo methods, the following constant ratios are normally determined in order to choose the appropriate fluid movement criteria (capillary, viscous or gravity domination).

Equations (1-7) and (1-8) are capillary to viscous number equation and gravity to viscous number equation respectively.

$$N_{pc/\mu} = \frac{k_v.\Delta pc.L}{k_h.\Delta p.h}$$

(1-7)

Capillary to viscous number

$$N_{\rho/\mu} = \frac{k_v \Delta \rho g \cos \alpha L}{k_h \Delta p}$$

(1-8)

Gravity to viscous number

Another parameter to be determined is the vertical equilibrium (VE) number, which indicates the dominated redistribution of the fluid in dip normal direction compared to the fluid movement in the areal directions, equation (1-9).

$$N_{VE} = N_{\rho/\mu} + N_{pc/\mu} \qquad \text{(1-9)}$$

Vertical equilibrium number

The fluid in the reservoir will be vertically segregated when the VE number is considerably larger than one and the capillary to viscous number is significantly smaller than one. In that case, the Coats' method can be applied with zero capillary pressure. It is applied for reservoirs with two or three phases. It assumes that the intermediate phase (second phase for a two phase reservoir) is a reference phase of capillary pressure (usually oil phase).

The following table summaries the criteria of selection for the appropriate static pseudo method.

Method	Criteria
Coats	Vertical equilibrium, segregated flow ($N_{VE} > 1$, $N_{pc/\mu} < 1$)
Hearn	Vertical communication , piston like displacement, viscous dominated ($N_{\rho g/\mu} < 1$)
Stiles	No communication , piston like displacement, mobility ratio = 1 ($N_{VE} < 1$)
Dykstra/Parson	As Stiles, mobility ratio not equal to 1 ($N_{VE} < 1$)

Coats started the static pseudo method with the assumptions of vertical equilibrium and segregated flow (i.e Vertical equilibrium number > 1 and capillary to viscous number < 1).

For a reservoir with good vertical communication with in layers and dominated by viscous force (small gravity to viscous number), there should be a 'piston like' displacement in each layer. In this case, the Hearn method is suitable for use.

In the case where a reservoir has low permeability and/or a barrier to vertical flow (non-communication within reservoir layers), it may have a vertical fluid distribution

that is independent of gravity and capillary effects. The displacement process in these types of reservoirs will be characterized by a small value of vertical equilibrium number. When displacement is piston like and the mobility ratio is equal to one, the Stiles' method can be used to generate pseudo relative permeability. For mobility not equal to one (no restriction with mobility ratio), the Dykstra/Parson method, which is an extension of Stiles' method, can then be used [8].

1.3.3.2   Dynamic Pseudo Method

In single-phase flow, the most important parameter to scale up is absolute permeability, and methods for this are well established. When multiphase flow occurs, however, it is also necessary to adjust the phase flow through the connections of the coarse grid. In such cases, the most widely used upscaling technique uses pseudo-relative permeabilities. The Kyte and Berry[12] method is the most common approach applied to calculate pseudo curves. Their procedure requires two steps: (1) generation of pseudocurves for each block of the coarser grid and (2) simulation of the model considering such functions. In addition to these generation steps, limitations associated to these pseudocurves restrict their use in a more general way. The procedure that Kyte and Barry used proposes uses parameters generated from numerical flow simulation in some regions of the domain to create an equivalence between the description and the simulation scales. By solving a sequence of local problems on the more refined scale, it is possible to achieve good agreement between a coarse and a fine grid without expensive computations on a fine-grid model of the whole reservoir. This procedure does not use multiphase pseudofunction concepts and avoids the computational cost of solving the fine grid. Simplified numerical and analytical models can be used to construct pseudofunctions. Analytical methods are suitable when simplified assumptions are valid.

To obtain the dynamic functions for each coarse block, it is necessary to run numerical models in a section of the reservoir. Jacks et al.[12] proposed a method based on simulation of 2D cross sections that generates a set of pseudo relative permeability curves representing each column and runs the final model in a 2D areal model.

Kyte and Berry proposed the most common method to calculate dynamic pseudo curves. They developed a method based on Darcy's law to calculate pseudofunctions that is considered to be an extension of Jacks et al.'s [12] work and includes pseudocapillary pressure curves. Despite the fact that their method is popular and used as a reference, it does not give good results in strongly heterogeneous media and some inconsistencies, such as negative or infinite values of relative permeability, can occur. On the basis of the Kyte and Berry approach, Lasseter et al. [12] presented a multiscale upscaling method suitable for heterogeneous reservoirs. Using some particular reservoir permeability distributions, they showed how reservoir heterogeneities at small, medium, and large scales influence ultimate recovery and how they affect the multiphase behavior. Lasseter et al.'s proposed pseudofunction-generation process begins at the laboratory scale, and the next largest scale can be achieved by replacing effective properties determined at the previous scale.

Stone[12] was the first to use the average total mobility to avoid calculating phase potential on the coarser grid (as required by the Kyte and Berry method). He introduced a fractional-flow formula instead of calculating the flow terms by Darcy's law. His method can be applied even to noncommunicating layers [12].

1.3.3.3   Capillary Equilibrium Limit and Viscous Limit Pseudo Methods

The other two common pseudo methods are the 'Capillary equilibrium limit' and 'viscous limit' methods. The Capillary equilibrium limit method is based on the assumption that the capillary pressure is in equilibrium within the coarse scale block that to be upscaled, while the viscous limit method is based on the assumption that the flow rate is large and viscous in terms that the flow equations dominate the flow. The fraction between the oil and water flow rate is assumed to be constant for all fine scale blocks within a coarse scale grid block and this determines implicitly that the water saturation for all fine scale grid blocks are in the coarse scale block. Upscaling is done by calculating the fine scale water saturation for different constant values of

capillary pressure, and water to oil flow fractions for the Capillary equilibrium and viscous limit method, respectively.

1.3.3.3.1   Capillary Equilibrium Limit Method

The capillary equilibrium limit method is based on the assumption that the capillary pressure is in equilibrium within the coarse scale block that is to be upscaled. This is true for sufficiently slow flow velocity, where the capillary pressure changes so slowly within space and can assumed to be constant over a volume corresponding to the size of grid block used in the reservoir fluid flow simulation.

The capillary pressure is then treated to be constant for all fine scale grid blocks within the coarse scale block. For any given capillary pressure value with the corresponding water saturation, the water saturation can then be used to determine the fine scale water and oil phase permeability, where phase permeability is the product of relative permeability and absolute permeability. The fine scale water and oil phase permeability for a given saturation distribution at the fine scale can then be scaled up using the same techniques as if they were absolute permeability. Diagonal tensor is often used to solve the incompressibility stationary one phase flow equation locally within the coarse grid block. The water saturation in the coarse block is scaled up by using the porosity weighted arithmetic average of the fine scale saturation. Different points on the upscaled relative permeability curves are then found by choosing different values of capillary pressure.

In summery, the upscaled relative permeability is a function of the capillary pressure, which corresponds to the upscaled critical saturations with the corresponding relative permeability values. The end point of the upscaled relative permeability is then based on the binary search of upscaled end points for the capillary pressures. The relative permeability of water at water saturation should be between zero and the specified tolerance [8].

1.3.3.3.2 Viscous Limit Method

This method assumes that the capillary pressure is zero ~ or negligibly small. At steady-state, the water saturation in each grid block of the model is constant with time.

This means that the fractional flow, fw going into and out of each block must be constant. When the capillary pressure is zero, the fractional flow may easily be calculated from the relative permeabilities, equation (1-10).

$$fw = \frac{k_{rw}\mu_o}{k_{rw}\mu_o + k_{ro}\mu_w} \tag{1-10}$$

Once again, the method is outlined here for completeness:

1. Select a fractional flow level, fw .

2. Calculate Sw by inverting the fw (Sw) function.

3. Calculate the average water saturation using pore-volume weighting.

4. Calculate the relative permeabilities and then the total mobility,

$$\lambda_t = k_{ro}/\mu_o + k_{rw}/\mu_w \tag{1-11}$$

5. Perform a single-phase simulation to calculate the effective total mobility.

6. Calculate the effective relative permeabilities using the formulas

$$\overline{k}_{rw} = \mu_w \overline{\lambda_t} fw / \overline{k}_{abs} \tag{1-12}$$

$$\overline{k}_{ro} = \mu_o (1 - fw)\overline{\lambda_t} / \overline{k}_{abs} \tag{1-13}$$

Where the overbears denote scaled-up values.

7. Repeat using a different value of the fractional flow to build a set of effective relative permeability curves. Tests of this method show that it works well [13].

Chapter 2

2 Results and Observation

2.1 Up-scaling Scenarios

The models were upscaled using **PETREL^{TM}** (**Schlumberger Package**); the upscaling procedures were done in horizontal and in vertical direction for different models.

By building the fine model geometry in the Petrel^{TM}, the properties of the fine model (porosity and permeability) can be assigned into each block.

The fine model has a simple geometry with no top structure or faults. The fine scale model consists of 1.122 x 10^6 cells (60x220x85). The model dimensions are 1200 x 2200 x 170 ft, where the top 70 ft (35 layers) represents the Tarbert formation, and the bottom 100 ft (50 layers) represents Upper Ness. The fine scale cell size is 20x10x2 ft [1][14][15][16].

The geometries of Up-scaled models will be created before starting upscaling the properties (porosity and permeability). The numbers of the up-scaled models were five models, the finest up-scaled model contains 280,500 cells, and the coarsest model contains 14,960 cells.

The I direction was up-scaled from 60 to 30 and 20, and for the J direction was set from 220 to 110, 55 and 44, and for K direction was set from 85 to 17.

Two algorithms were used to upscale the permeability, analytical and numerical. From the analytical algorithm the harmonic method was chosen, and from the numerical algorithms the diagonal tensor method was selected. The porosity was upscaled by analytical algorithms (arithmetically), and these results into 10 scenarios, 5 for each algorithm represent the new geometry and the new properties.

These models were exported to **Eclipse (Schlumberger Package)** to start the dynamic flow and to start the investigation. Thus a total of 10 runs were performed, and the quality of the scale-up was assessed by comparing the scaled-up grid performance with the fine grid performance [14][15].

2.2 Models

2.2.1 Fine Model

The fine model consist of 60 grid in I direction, 220 in J direction and 85 in K direction with total number of grids 1.122 x 10^6.

The fine model was the reference model for the other five models, whereas the grids were upscaled in I, J and K directions. The properties of the model were assigned using Petrel^{TM} and no dynamic simulation was done to this model due to the large number of cells (time consuming) [14][15][16].

2.2.2 Model 1

This model consist of 60 grid in I direction, 55 in J direction and 85 in K direction with total number of grids 280,500.

Two different 1D scale ups algorithms (analytical and numerical) were preformed for each model to compare the two different scale-up methods. For model 1 the geometry was scaled up in J direction only form 220 to 55.The K (vertical) and I (areal) directions were remained fixed. The two scenarios were exported to Eclipse to perform the simulation run.

2.2.3 Model 2

This model consist of 30 grid in I direction, 55 in J direction and 85 in K direction with total number of grids 140,250.

Two different 1D scale ups algorithms (analytical and numerical) were preformed to compare the two different scale-up methods. For model 2 the geometry was scaled up in I and J direction from 60 to 30 for I direction and form 220 to 55 in J direction. The K (vertical) direction was remained fixed. The two scenarios were exported to Eclipse to perform the simulation run.

2.2.4 Model 3

This model consist of 30 grid in I direction, 110 in J direction and 17 in K direction with total number of grids 56,100.

Two different 1D scale ups algorithms (analytical and numerical) were preformed to compare the two different scale-up methods. For model 3 the geometry was scaled up in I , J and K directions from 60 to 30 for I direction, and form 220 to 110 in J direction, and from 85 to 17 in K direction. The two scenarios were exported to Eclipse to perform the simulation run.

2.2.5 Model 4

This model consist of 30 grid in I direction, 44 in J direction and 17 in K direction with total number of grids 22,440.

Two different 1D scale ups algorithms (analytical and numerical) were preformed to compare the two different scale-up methods. For model 4 the geometry was scaled up in I , J and K directions from 60 to 30 for I direction, and form 220 to 44 in J direction, and from 85 to 17 in K direction. The two scenarios were exported to Eclipse to perform the simulation run.

2.2.6 Model 5

This model consist of 20 grid in I direction, 44 in J direction and 17 in K direction with total number of grids 14,960.

Two different 1D scale ups algorithms (analytical and numerical) were performed to compare the two different scale up method , and for model 5 the geometry was scaled up in I , J and K directions ,from 60 to 20 for I direction and form 220 to 44 in J direction and from 85 to 17 in K direction. The two scenarios were exported to Eclipse to perform the simulation run.

Table (2-1), (2-2) and (2-3) shows over view on the six models (five coarsened models with the fine model), it gives the limitation of the porosity and permeability range. Also it shows the total pore volume after running the dynamic model and, the dimension of all the models are also shown.

Table 2-1: The Porosity and size limitation.

Models	Cells in			Total Cells	porosity		Total Pore Volume
	I	J	K		Min	Max	RB
fine model	60	220	85	1.122.000	0	0,5	
model 1	60	55	85	280.500	0	0,478	13.636.60
model 2	30	55	85	140.250	0	0,472	13.636.60
model 3	30	110	17	56.100	0	0,37	13.636.60
model 4	30	44	17	22.440	0	0,367	13.636.60
model 5	20	44	17	14.960	0	0,367	13.636.60

Table 2-2: The Permeability in the Analytical method and size limitation.

Models	Cells in			Total Cells	permeability (Ana.), md					
	I	J	K		X		Y		Z	
					Min	Max	Min	Max	Min	Max
Fine model	60	220	85	1122000	0	20000	0	20000	0	20000
model 1	60	55	85	280.500	0	15589	0	15772	0	3925
model 2	30	55	85	140.250	0	14716	0	15633	0	3112
model 3	30	110	17	56.100	0	11513	0	11633	0	1600
model 4	30	44	17	22.440	0	9282	0	8370	0	1258
model 5	20	44	17	14.960	0	8996	0	8210	0	1122

Table 2-3: The Permeability in the Numerical method and size limitation.

Models	Cells in			Total Cells	permeability (Num.), md					
	I	J	K		X		Y		Z	
					Min	Max	Min	Max	Min	Max
model 1	60	55	85	280.500	0	15589	0	15772	0	3925
model 2	30	55	85	140.250	0	14716	0	15633	0	3112
model 3	30	110	17	56.100	0	11513	0	11633	0	1600
model 4	30	44	17	22.440	0	9282	0	8370	0	1258
model 5	20	44	17	14.960	0	8996	0	8210	0	1122

2.3 Analysis of the Results

After completing the upscaling in Petrel[TM] for all the models, the models are exported to Eclipse to perform the dynamic flow simulation.

The initial conditions for the simulation models were set as the following:

- Initial pressure is 6000 psi at reference depth 12000 ft.
- One injector with Injection rate 5000 bbl/day (reservoir condition).
- Max injection bottom hole pressure 10000 psi.
- Four producers, produces at 4000 psi bottom hole pressur.
- The model is simulated for 2000 day [14][15][16].
- The time step length is 3 month.

The details are found in Appendix B.

2.3.1 Comparison of Field Oil Production Rate (FOPR) for Different Upscaling Models.

The Result of Upscaling Indicated the Following:

Analytical Method:

- Model 1 and 2 with dimensions of (60x55x85) (30x55x85) respectively , showed a drop 500 stb/day from the fine model which was 5000 stb/day at 120 day of production, and along the production period they showed good match to the fine model , although a small different occur between 400 to 800 days.
- The reset of the models which are model 3, model 4 and model 5 with dimensions of (30x110x17),(30x44x17) and (20x44x17) respectively did not show good match with the fine model , although they were matched well together, they showed over estimation for the daily field production.
- After 1120 day all models showed good match with the fine model (Figure 2-1), (Table 2-4).

Numerical Method:

- All the models showed a perfect overall field performance, and they matched the fine model perfectly (Figure 2-2), (Table 2-5).

- The original oil in place OOIP ,was the same in both method 10,772,610 STB

Table 2-4: Comparison of FOPR at different Upscaling (Analytical method).

Date	Days	Fine M. Days	Fine M. 60X220X85 FOPR Field STB/DAY	Model 1 60X55X85 FOPR Field STB/DAY	Model 2 30X55X85 FOPR Field STB/DAY	Model 3 30X110X17 FOPR Field STB/DAY	Model 4 30X44X17 FOPR Field STB/DAY	Model 5 20X44X17 FOPR Field STB/DAY
01.Jän.90								
01.Mai.90	120	120	4900	4486,829	4521,134	4910,892	4913,825	4914,054
01.Sep.90	243	200	3600	3294,119	3364,369	4274,475	4414,538	4500,72
01.Jän.91	365	300	2800	2284,905	2309,479	3347,059	3418,882	3433,639
01.Mai.91	485	400	2200	1743,982	1762,388	2565,039	2559,676	2594,991
01.Sep.91	608	600	1700	1421,893	1425,061	2014,745	2033,347	2051,89
01.Jän.92	730	800	1200	1206,489	1203,334	1647,151	1670,243	1682,331
01.Mai.92	851	1000	1000	1048,6	1048,319	1386,47	1407,264	1425,861
01.Sep.92	974	1200	900	924,6237	930,0662	1189,081	1207,418	1225,572
01.Jän.93	1096	1400	800	830,0425	835,6695	1042,038	1059,376	1077,587
01.Mai.93	1216	1600	700	754,5947	756,0024	931,8841	947,3628	961,8135
01.Sep.93	1339	1800	600	691,1451	692,2681	842,1552	855,1938	868,6435
01.Jän.94	1461	2000	500	637,9999	639,287	769,7222	780,5779	791,9372
01.Mai.94	1581			592,9008	594,5574	710,2028	719,4603	729,955
01.Sep.94	1704			553,1683	554,913	658,3347	666,5595	675,7629
01.Jän.95	1826			518,9633	520,9203	614,1979	621,9139	630,3285
01.Mai.95	1946			489,6023	491,4977	576,3179	583,9458	592,1779
01.Jul.95	2007			475,9171	477,7693	558,9069	566,505	574,3913

Figure 2-1: Comparison of FOPR at different Upscaling (Analytical method).
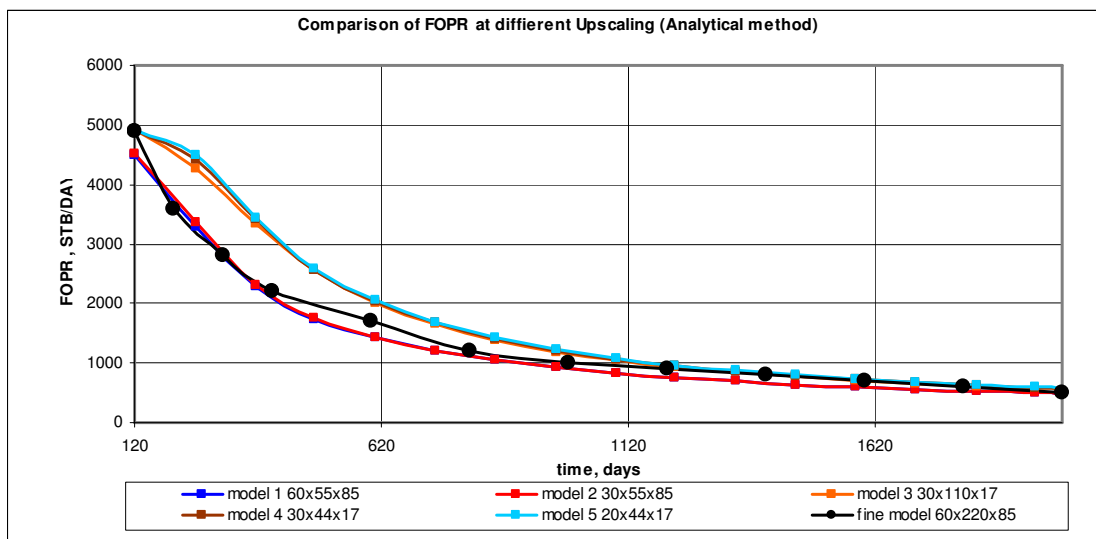
Table 2-5: Comparison of FOPR at different Upscaling (Numerical method).

Date	Days	Fine M. Days	Fine M. 60X220X85 FOPR Field STB/DAY	Model 1 60X55X85 FOPR Field STB/DAY	Model 2 30X55X85 FOPR Field STB/DAY	Model 3 30X110X17 FOPR Field STB/DAY	Model 4 30X44X17 FOPR Field STB/DAY	Model 5 20X44X17 FOPR Field STB/DAY
01.Jän.90								
01.Mai.90	120	120	4900	4568,033	4618,922	4732,907	4758,078	4809,313
01.Sep.90	243	200	3600	3471,993	3543,873	3440,514	3518,34	3559,527
01.Jän.91	365	300	2800	2470,747	2500,542	2527,512	2610,847	2665,932
01.Mai.91	485	400	2200	1893,858	1928,52	1939,379	2010,409	2075,568
01.Sep.91	608	600	1700	1526,763	1552,779	1566,003	1623,575	1674,681
01.Jän.92	730	800	1200	1294,382	1313,715	1325,131	1376,025	1401,918
01.Mai.92	851	1000	1000	1118,412	1136,963	1158,005	1192,902	1218,173
01.Sep.92	974	1200	900	989,4698	1002,983	1021,631	1056,903	1078,893
01.Jän.93	1096	1400	800	887,5425	900,0976	922,0956	950,4057	973,4354
01.Mai.93	1216	1600	700	805,2722	817,0748	840,599	866,8404	885,687
01.Sep.93	1339	1800	600	737,2332	747,2923	773,6713	797,1665	813,0685
01.Jän.94	1461	2000	500	680,5609	688,787	714,3484	739,084	751,8749
01.Mai.94	1581			631,5162	639,3876	667,2945	688,7717	700,7581
01.Sep.94	1704			588,2839	595,559	623,7369	644,2681	655,2812
01.Jän.95	1826			551,5883	558,0588	587,8497	604,8813	615,0523
01.Mai.95	1946			519,6949	525,6821	557,5734	569,8954	578,8799
01.Jul.95	2007			504,5928	510,447	543,4713	553,248	561,4277

Figure 2-2: Comparison of FOPR at different Upscaling (Numerical method).
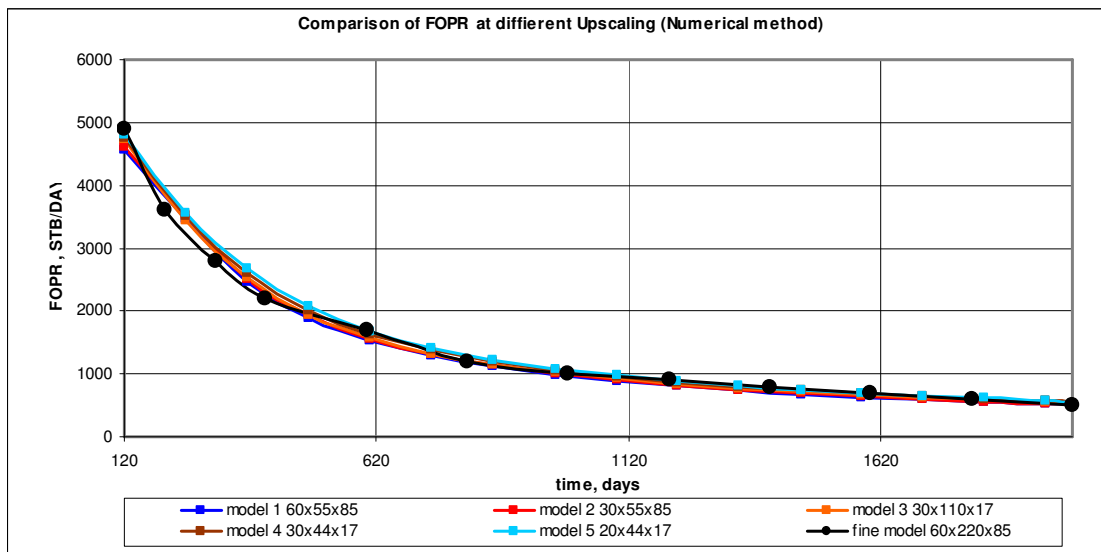
2.3.2 Comparison of Oil Production Rate (WOPR) for Well P1 at Different Upscaling Models.

Analytical Method:

- All the wells showed discrepancies at early time, thus all the models started at 120 days to avoid this search rate.
- The largest models model 1 and model 2 with dimensions of (60x55x85) (30x55x85) respectively showed good match to the fine model starting form the 120 day until the end of simulation period which is 2000 day.
- The other 3 models consist of much coarsest grid than the first 2, and the behavior of the 3 coarsest models model 3 , model 4 and model 5 with dimensions of (30x110x17), (30x44x17) and (20x44x17) respectively showed much higher production nearly overall the period (from 120 day to 1461 day), and that could be caused by high reduction in cells number from 1.122 million cell (fine model) to 56.100 cell for model 3 , 22.440 cell for model 4 and 14.960 cell for model 5. The 3 models showed the maximum diverge from the fine model at 365 day, and start to come down until it matched the fine model at 1461 day (Figure 2-3), (Table 2-6).

Numerical Method:

- All the models performances were in a very good agreement with the fine model performance, although there was a small overestimation for all the models in the first period (from 120 day to 800 day).
- Model 1, 2 and 3 was the closest to the fine model (Figure 2-4), (Table 2-7).
- The original oil in place OOIP ,was the same in both method 10,772,610 STB

Table 2-6: **Comparison of WOPR for Well P1 at different Upscaling (Analytical model).**

Date	Days	Fine M. Days	Fine M. 60X220X85 WOPR P1 STB/DAY	Model 1 60X55X85 WOPR P1 STB/DAY	Model 2 30X55X85 WOPR P1 STB/DAY	Model 3 30X110X17 WOPR P1 STB/DAY	Model 4 30X44X17 WOPR P1 STB/DAY	Model 5 20X44X17 WOPR P1 STB/DAY
01.Jän.90								
01.Mai.90	120	120	700	604,5943	649,662	735,7342	754,5451	753,2927
01.Sep.90	243	150	620	522,3641	550,28	705,2178	737,887	739,8776
01.Jän.91	365	200	570	368,9487	388,0751	632,0295	647,9978	638,1231
01.Mai.91	485	300	480	286,5875	304,3721	496,3225	503,5659	495,0307
01.Sep.91	608	400	360	239,3624	252,6188	386,2729	407,7096	395,7991
01.Jän.92	730	600	260	209,5942	218,1224	319,9681	332,9631	325,2585
01.Mai.92	851	800	220	188,1576	193,9039	267,791	278,9388	275,7271
01.Sep.92	974	1000	180	169,4978	174,9279	230,682	236,3175	236,1263
01.Jän.93	1096	1200	160	154,798	158,7903	203,5447	207,12	207,1924
01.Mai.93	1216	1400	150	142,8851	146,3556	183,1458	185,9897	184,918
01.Sep.93	1339	1600	130	132,663	135,8337	166,5391	168,7025	167,6149
01.Jän.94	1461	1800	120	123,9223	126,8054	153,1444	154,9794	153,4431
01.Mai.94	1581	2000	100	116,386	118,9395	142,2592	143,8349	142,062
01.Sep.94	1704			109,5756	112,1017	132,8328	134,1779	132,0969
01.Jän.95	1826			103,4848	106,0925	124,8049	125,986	123,8205
01.Mai.95	1946			98,2557	100,6773	117,9118	118,9923	116,8702
01.Jul.95	2007			95,78091	98,0919	114,7355	115,762	113,5929

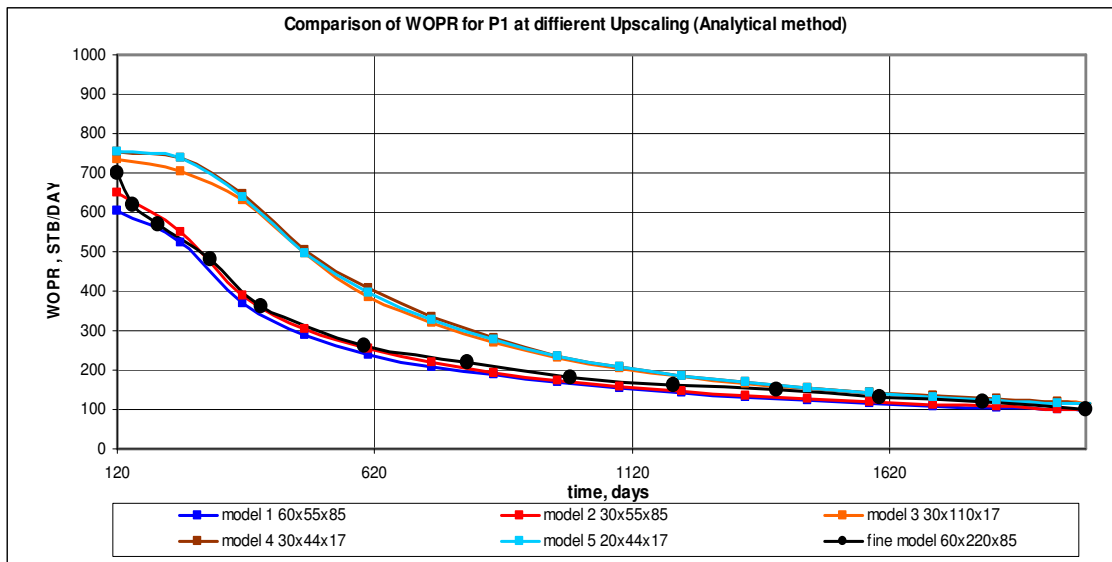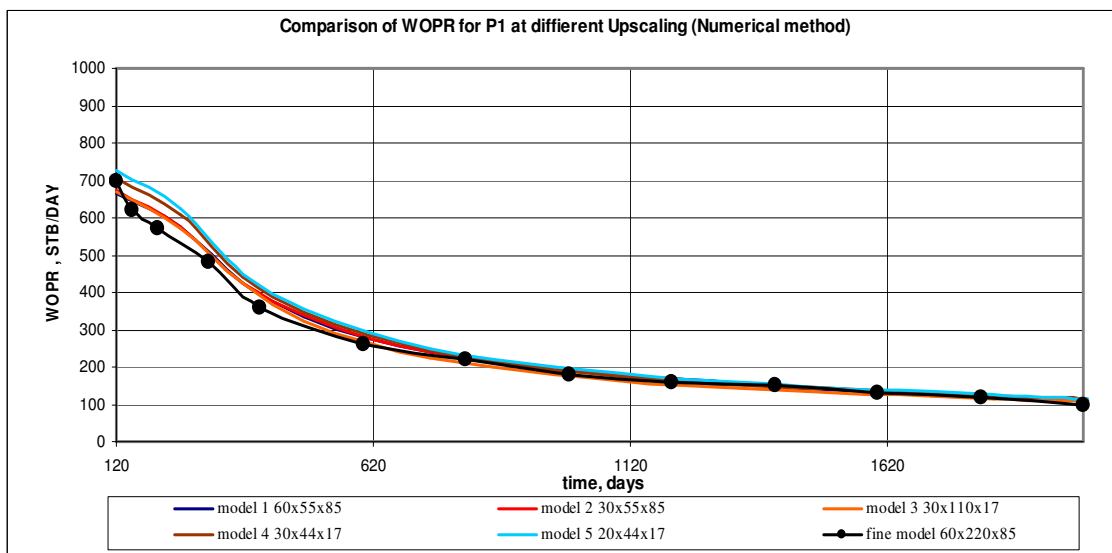**Figure 2-3:** **Comparison of WOPR for Well P1 at different Upscaling (Analytical model).**

Table 2-7: Comparison of WOPR for Well P1 at different Upscaling (Numerical model).

Date	Days	Fine M. Days	Fine M. 60X220X85 WOPR P1 STB/DAY	Model 1 60X55X85 WOPR P1 STB/DAY	Model 2 30X55X85 WOPR P1 STB/DAY	Model 3 30X110X17 WOPR P1 STB/DAY	Model 4 30X44X17 WOPR P1 STB/DAY	Model 5 20X44X17 WOPR P1 STB/DAY
01.Jän.90								
01.Mai.90	120	120	700	667,1493	672,5095	668,1606	707,2054	724,5482
01.Sep.90	243	150	620	574,2684	574,9523	572,8948	609,6558	622,9828
01.Jän.91	365	200	570	425,8775	423,4076	424,2731	441,4163	447,9822
01.Mai.91	485	300	480	336,456	339,6875	324,006	348,8688	354,5227
01.Sep.91	608	400	360	276,1084	278,3732	263,3703	285,5741	293,1675
01.Jän.92	730	600	260	240,0018	240,6319	225,9806	244,6145	249,3342
01.Mai.92	851	800	220	214,6362	214,9017	199,3007	215,0367	220,5278
01.Sep.92	974	1000	180	195,3515	195,0052	180,0759	193,388	198,4726
01.Jän.93	1096	1200	160	179,3223	179,3828	164,9874	176,6322	181,911
01.Mai.93	1216	1400	150	165,5484	166,6072	152,3835	163,8483	168,5081
01.Sep.93	1339	1600	130	154,1464	155,1767	142,2038	153,0291	157,3855
01.Jän.94	1461	1800	120	144,5383	145,2635	133,9119	144,1884	148,0881
01.Mai.94	1581	2000	100	135,2763	136,0988	127,051	136,8232	140,3612
01.Sep.94	1704			126,7834	127,5144	121,023	130,2194	133,3259
01.Jän.95	1826			119,8126	120,1282	115,8395	124,132	126,6474
01.Mai.95	1946			113,4975	113,662	111,2822	117,8797	119,6996
01.Jul.95	2007			110,4307	110,5541	108,9778	114,7456	116,0854

Figure 2-4: Comparison of WOPR for Well P1 at different Upscaling (Numerical model).

2.3.3 Comparison of Total Oil Production (WOPT) for Well P1 at different Upscaling models.

Analytical Method:

- Model 1 (60x55x85) and model 2 (30x55x85) was in a very good agreement with the fine model performance
- The three coarsest models model 3, model 4 and model 5 with dimensions of (30x110x17), (30x44x17) and (20x44x17) respectively overestimated the total well P1 oil production. This overestimation has increased with time until it reached 670,000 STB were it should be 470,000 STB (fine model) after 1800 day of production (Figure 2-5), (Table 2-8).

Numerical Method:

- All the models nearly started at the same production with the fine model. The loss of accuracy started to increase gradually with time, although all the models were near to the fine model.
- There was a small over estimation for all the models, however model 3 with dimension of (30x110x17) was the closest because the upscaling in Y direction was not so high just form 220 cell to 110 cell (Figure 2-6), (Table 2-9).
- The original oil in place OOIP ,was the same in both method 10,772,610 STB

Table 2-8: Comparison of WOPT for Well P1 at different Upscaling (Analytical model).

Date	Days	Fine M. Days	Fine M. 60X220X85 WOPT P1 STB	Model 1 60X55X85 WOPT P1 STB	Model 2 30X55X85 WOPT P1 STB	Model 3 30X110X17 WOPT P1 STB	Model 4 30X44X17 WOPT P1 STB	Model 5 20X44X17 WOPT P1 STB
01.Jän.90								
01.Mai.90	120	120	80000	82064,77	88614,98	98285,52	101115,9	101021,1
01.Sep.90	243	200	120000	152277,5	163688,5	187311,2	193105	193032,5
01.Jän.91	365	300	180000	206140,9	220191,3	268780,8	277374,4	276979,2
01.Mai.91	485	400	220000	244904,5	261130,3	336697,2	345324,9	340337,7
01.Sep.91	608	600	260000	276976,7	295124,6	389986,2	400148,8	391786,6
01.Jän.92	730	800	320000	304218,2	323676,2	432470,5	444583,8	434560,9
01.Mai.92	851	1000	360000	328227,2	348521,8	467749,3	481105,6	469306,3
01.Sep.92	974	1400	420000	350169	371146,6	498097,5	512338,2	500148,5
01.Jän.93	1096	2000	480000	369903,9	391456,4	524371,3	539070,1	526247
01.Mai.93	1216			387742,3	409735,2	547415,6	562385,8	549407,6
01.Sep.93	1339			404657	427062,7	568781,2	584031,6	570526,8
01.Jän.94	1461			420292,8	443070,9	588160,8	603591,8	589884
01.Mai.94	1581			434695,3	457797	605801,7	621385,2	607258,9
01.Sep.94	1704			448580	471991,8	622649,1	638363,1	623961,2
01.Jän.95	1826			461564	485291,7	638296,5	654133,6	639310,1
01.Mai.95	1946			473658,4	497689,4	652804,9	668749,8	653334,5
01.Jul.95	2007			479574,1	503749,8	659882,6	675886,1	660263,7

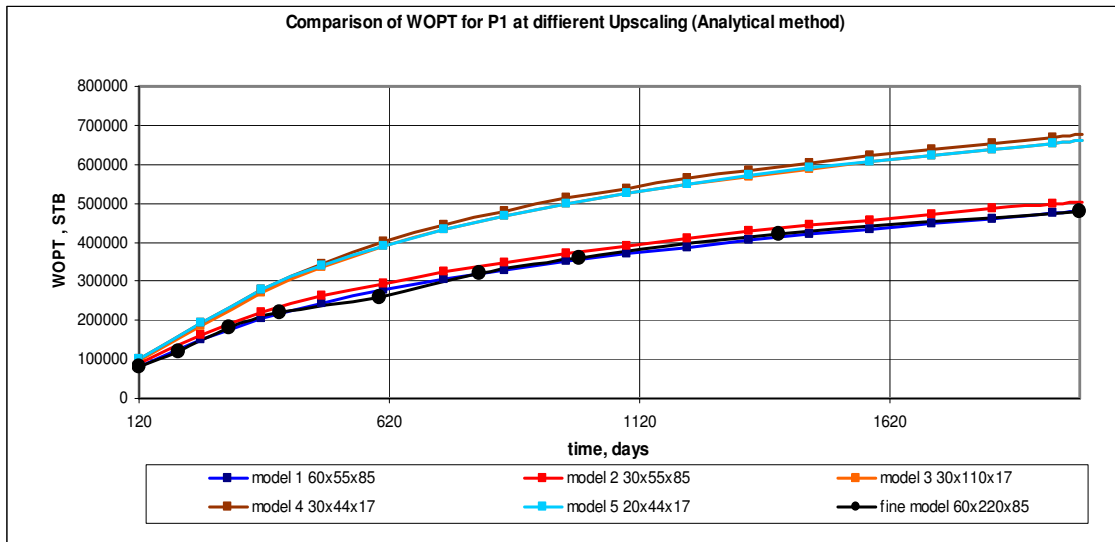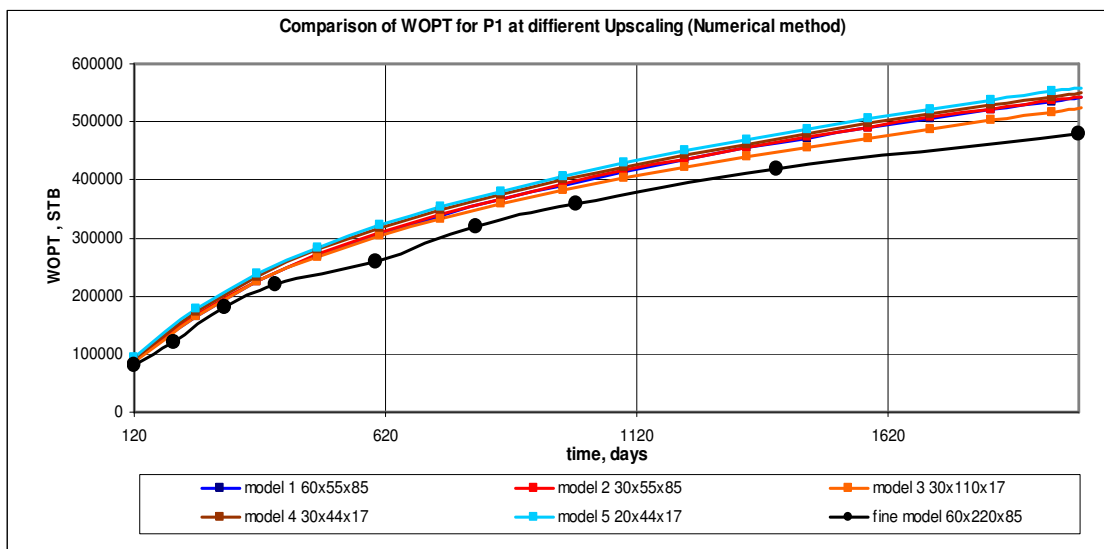**Figure 2-5: Comparison of WOPT for Well P1 at different Upscaling (Analytical model).**

Table 2-9: Comparison of WOPT for Well P1 at different Upscaling (Numerical model).

Date	Days	Fine M. Days	Fine M. 60X220X85 WOPT P1 STB	Model 1 60X55X85 WOPT P1 STB	Model 2 30X55X85 WOPT P1 STB	Model 3 30X110X17 WOPT P1 STB	Model 4 30X44X17 WOPT P1 STB	Model 5 20X44X17 WOPT P1 STB
01.Jän.90								
01.Mai.90	120	120	80000	88219,93	88874,48	87322,4	92096,8	94513,1
01.Sep.90	243	200	120000	165565,5	166723,8	163780,3	172407,3	177224,6
01.Jän.91	365	300	180000	225125,7	225855,3	224595,5	234337	238449
01.Mai.91	485	400	220000	270583,2	271207,3	268535,9	279901,2	283417,8
01.Sep.91	608	600	260000	307803,9	308726,6	304126	317696,3	321198,7
01.Jän.92	730	800	320000	339103,8	340124,3	333710,4	348675,5	353506,2
01.Mai.92	851	1000	360000	366510,2	367529	359221,7	375982,2	380988,2
01.Sep.92	974	1400	420000	391645,2	392621,5	382416,3	400388,3	406385,8
01.Jän.93	1096	2000	480000	414463,8	415390,1	403364,3	422682,8	429053,9
01.Mai.93	1216			435102,3	436091,1	422329,8	442708,8	449868,2
01.Sep.93	1339			454730,9	455818,4	440376,5	462022,1	469554
01.Jän.94	1461			472923,6	474108,5	457173,2	479971,8	488040,9
01.Mai.94	1581			489694,3	490952,9	472786,2	496674	505107,7
01.Sep.94	1704			505772,7	507125,9	488007,6	512889,1	521832,7
01.Jän.95	1826			520795,3	522194,3	502431,3	528318,1	537488,3
01.Mai.95	1946			534778,6	536192,4	516029,8	542652,4	551852,2
01.Jul.95	2007			541602,2	543012,3	522739,2	549651,9	558933,4

Figure 2-6: Comparison of WOPT for Well P1 at different Upscaling (Numerical model).

3-3-4 Comparison of Well Water Cut (WWCT) for Well P1 at Different Upscaling Models.

Analytical Method:

- Model 1 (60x55x85) and model 2 (30x55x85) was in a very good agreement with the fine model performance
- The three coarsest models model 3, model 4 and model 5 with dimensions of (30x110x17), (30x44x17) and (20x44x17) respectively underestimated the water cut for well P1. This underestimation has decreased with time until it matched the fine model after 974 day (Figure 2-7), (Table 2-10).

Numerical Method:

- All the models started with the fine model. The loss of accuracy started to increase gradually with time, although all the models were near to the fine model.
- Model 1 (60x55x85) and model 2 (30x55x85) fitted the fine model very well, although there where a small underestimation between 1340 day to 2000 day of 3%.
- Over estimation of the WWCT took place in the period between 500 days to 1500 day for model 3, model 4 and model 5 with dimensions of (30x110x17), (30x44x17) and (20x44x17) respectively , however all the models ended with the same percentage of WWCT (Figure 2-8), (Table 2-11).
- The original oil in place OOIP ,was the same in both method 10,772,610 STB

Table 2-10: Comparison of WWCT for Well P1 at different Upscaling (Analytical model).

Date	Days	Fine M. Days	Fine M. 60X220X85 WWCT P1 %	Model 1 60X55X85 WWCT P1 %	Model 2 30X55X85 WWCT P1 %	Model 3 30X110X17 WWCT P1 %	Model 4 30X44X17 WWCT P1 %	Model 5 20X44X17 WWCT P1 %
01.Jän.90	0	0	0	0	0	0	0	0
01.Mai.90	120	200		0,001551	0,001707	0,001911	0,001994	0,002014
01.Sep.90	243	300	0,08	0,017998	0,041554	0,001892	0,002114	0,002251
01.Jän.91	365	400	0,25	0,203919	0,235742	0,002916	0,027315	0,043958
01.Mai.91	485	600	0,42	0,359012	0,372123	0,124216	0,176549	0,205303
01.Sep.91	608	800	0,53	0,45247	0,467754	0,287808	0,307815	0,346906
01.Jän.92	730	1000	0,6	0,511671	0,533652	0,397187	0,421924	0,456919
01.Mai.92	851	1200	0,65	0,555769	0,581318	0,488546	0,513179	0,537893
01.Sep.92	974	1400	0,7	0,595532	0,619256	0,557714	0,586251	0,603442
01.Jän.93	1096	1600	0,74	0,627692	0,652488	0,610367	0,638189	0,652539
01.Mai.93	1216	1800	0,76	0,654433	0,678564	0,650107	0,675656	0,690073
01.Sep.93	1339	2000	0,8	0,678092	0,700849	0,682486	0,705971	0,719655
01.Jän.94	1461			0,69876	0,720124	0,708828	0,730215	0,743931
01.Mai.94	1581			0,716988	0,737291	0,730321	0,74997	0,763251
01.Sep.94	1704			0,733675	0,752496	0,748957	0,767064	0,779967
01.Jän.95	1826			0,748592	0,766097	0,764776	0,781507	0,79402
01.Mai.95	1946			0,761543	0,778519	0,77835	0,793783	0,805956
01.Jul.95	2007			0,767725	0,784486	0,784601	0,799454	0,811549

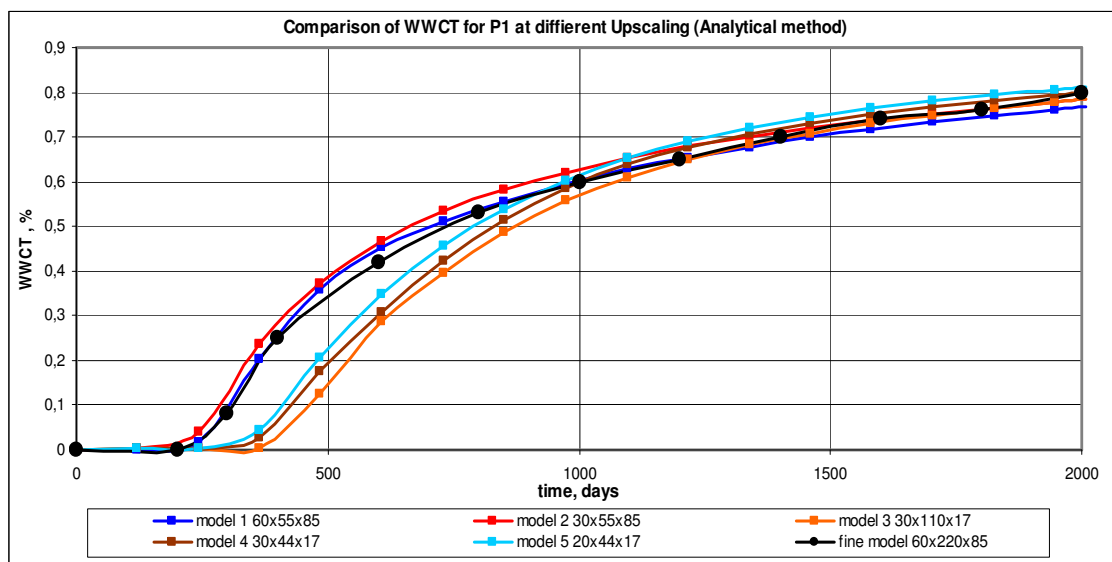**Figure 2-7: Comparison of WWCT for Well P1 at different Upscaling (Analytical model).**

Table 2-11: Comparison of WWCT for Well P1 at different Upscaling (Numerical model).

Date	Days	Fine M. Days	Fine M. 60X220X85 WWCT P1 %	Model 1 60X55X85 WWCT P1 %	Model 2 30X55X85 WWCT P1 %	Model 3 30X110X17 WWCT P1 %	Model 4 30X44X17 WWCT P1 %	Model 5 20X44X17 WWCT P1 %
01.Jän.90			0	0	0	0	0	0
01.Mai.90	120	200	0	0,001182	0,001242	0,001318	0,001367	0,001386
01.Sep.90	243	300	0,08	0,03146	0,037403	0,02441	0,013604	0,017339
01.Jän.91	365	400	0,25	0,207022	0,223863	0,200825	0,209008	0,237775
01.Mai.91	485	600	0,42	0,335384	0,343164	0,374834	0,36152	0,388335
01.Sep.91	608	800	0,53	0,435501	0,442411	0,485844	0,47199	0,488388
01.Jän.92	730	1000	0,6	0,499719	0,508192	0,556745	0,543152	0,562097
01.Mai.92	851	1200	0,65	0,545516	0,554535	0,609348	0,597452	0,611019
01.Sep.92	974	1400	0,7	0,581572	0,591097	0,647179	0,637902	0,649027
01.Jän.93	1096	1600	0,74	0,613962	0,621186	0,676784	0,668761	0,677968
01.Mai.93	1216	1800	0,76	0,642264	0,646796	0,701815	0,692308	0,701347
01.Sep.93	1339	2000	0,8	0,665835	0,670338	0,72239	0,712579	0,720938
01.Jän.94	1461			0,685979	0,690795	0,739193	0,729428	0,737454
01.Mai.94	1581			0,70557	0,709945	0,753022	0,743425	0,751222
01.Sep.94	1704			0,723869	0,728098	0,765107	0,755889	0,763771
01.Jän.95	1826			0,739016	0,743844	0,775464	0,767255	0,775669
01.Mai.95	1946			0,752861	0,757731	0,78453	0,778921	0,788011
01.Jul.95	2007			0,759676	0,764456	0,789099	0,784836	0,794429

Figure 2-8: Comparison of WWCT for Well P1 at different Upscaling (Numerical model).
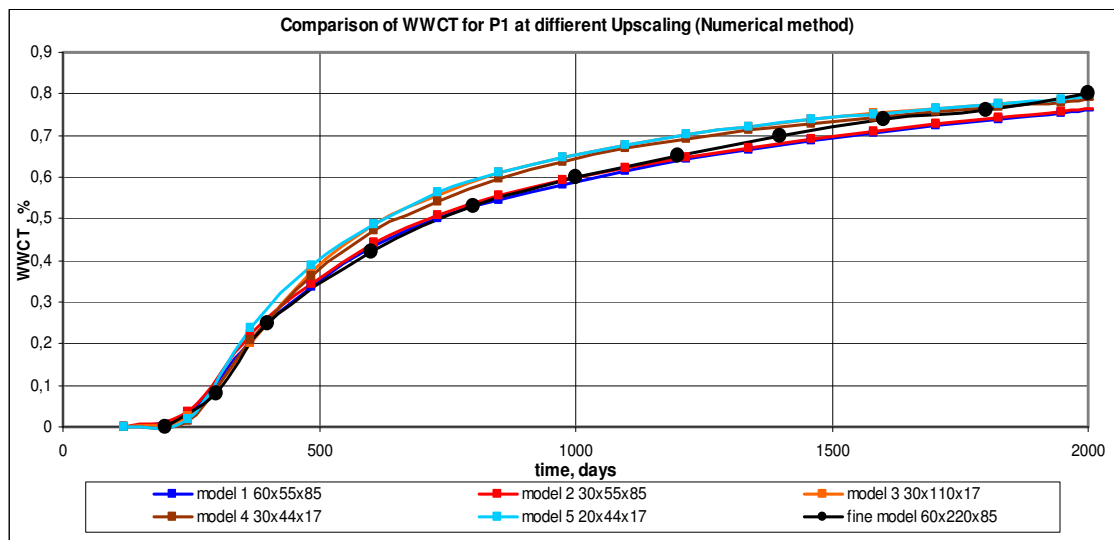
2.3.4   Comparison of Oil Production Rate (WOPR) for Well P3 at Different Upscaling Models.

Analytical Method:

- All the wells showed discrepancies at early time, thus all the models started at 120 days to avoid this search rate.
- The largest models model 1 and model 2 with dimensions of (60x55x85) (30x55x85) respectively showed good match to the fine model starting form the 120 day until the end of simulation period which is 2000 day.
- The other 3 models consist of much coarsest grid than the first 2, and the behavior of the 3 coarsest models model 3 , model 4 and model 5 with dimensions of (30x110x17), (30x44x17) and (20x44x17) respectively showed much higher production in the period from 120 day to 1120 day, and that could be caused by high reduction in cells number from 1.122 million cell (fine model) to 56.100 cell for model 3 , 22.440 cell for model 4 and 14.960 cell for model 5 (Figure 2-9), (Table 2-12).

Numerical Method:

- At 120 days there was overestimation to the daily production about 197 bbl for all the models; however this overestimation started gradually to decrease until it matched the fine model after 800 days and kept on this situation until the end of the production period.
- All the models performance were very tight to each other (identical) , and very close to the fine model (Figure 2-10), (Table 2-13).
- The original oil in place OOIP ,was the same in both method 10,772,610 STB

Table 2-12: Comparison of WOPR for Well P3 at different Upscaling (Analytical model).

Date	Days	Fine M. Days	Fine M. 60X220X85 WOPR P3 STB/DAY	Model 1 60X55X85 WOPR P3 STB/DAY	Model 2 30X55X85 WOPR P3 STB/DAY	Model 3 30X110X17 WOPR P3 STB/DAY	Model 4 30X44X17 WOPR P3 STB/DAY	Model 5 20X44X17 WOPR P3 STB/DAY
01.Jän.90								
01.Mai.90	120	120	1700	1806,303	1770,335	1980,328	1935,829	1869,542
01.Sep.90	243	200	1350	1250,476	1277,466	1539,625	1561,486	1569,895
01.Jän.91	365	300	1000	841,7955	847,3531	1111,189	1134,432	1127,292
01.Mai.91	485	400	800	628,9244	628,544	831,3546	837,2192	841,4287
01.Sep.91	608	600	500	502,4798	498,5135	649,4262	651,1462	653,6891
01.Jän.92	730	800	380	418,2396	414,5317	529,1407	533,5964	530,9457
01.Mai.92	851	1000	300	358,2284	356,2721	445,9596	451,1418	449,8727
01.Sep.92	974	1200	250	312,5509	311,72	383,0235	389,106	387,819
01.Jän.93	1096	1400	230	277,5409	276,9755	335,259	341,6846	341,1694
01.Mai.93	1216	1600	200	250,1616	249,1763	298,5857	304,9401	304,4111
01.Sep.93	1339	1800	180	227,3521	226,2604	268,5495	274,3023	274,2497
01.Jän.94	1461	2000	120	208,626	207,5388	244,2284	249,1787	249,3129
01.Mai.94	1581			193,1118	192,0345	224,3387	228,5845	228,8997
01.Sep.94	1704			179,5305	178,4561	207,0921	210,7337	211,0611
01.Jän.95	1826			167,8843	166,8541	192,4774	195,684	196,0176
01.Mai.95	1946			157,8449	156,9218	180,0023	182,9237	183,3725
01.Jul.95	2007			153,187	152,3439	174,2749	177,0643	177,5275

Figure 2-9: Comparison of WOPR for Well P3 at different Upscaling (Analytical model).
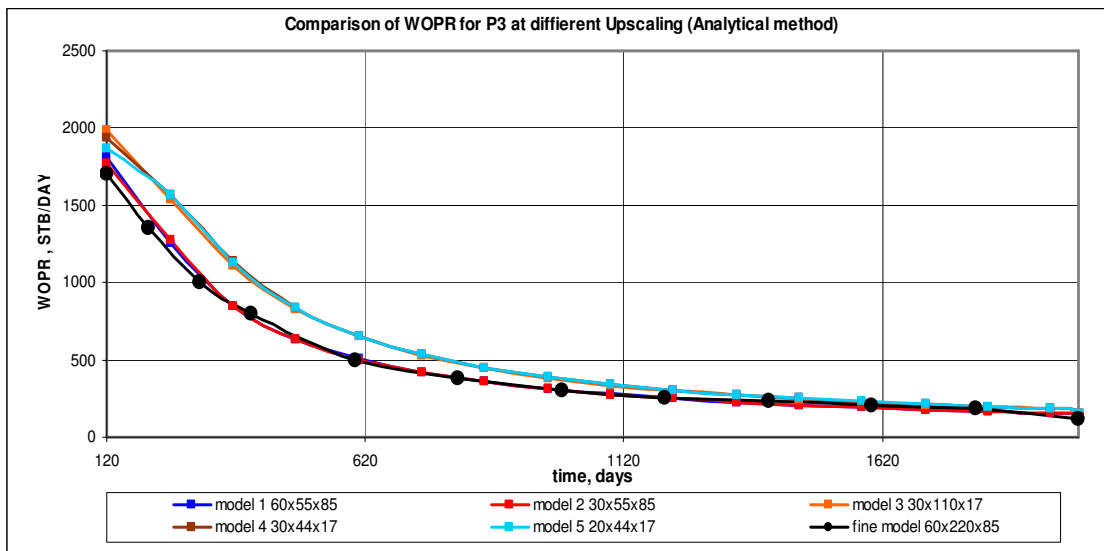
Table 2-13: Comparison of WOPR for Well P3 at different Upscaling (Numerical model).

Date	Days	Fine M. Days	Fine M. 60X220X85 WOPR P3 STB/DAY	Model 1 60X55X85 WOPR P3 STB/DAY	Model 2 30X55X85 WOPR P3 STB/DAY	Model 3 30X110X17 WOPR P3 STB/DAY	Model 4 30X44X17 WOPR P3 STB/DAY	Model 5 20X44X17 WOPR P3 STB/DAY
01.Jän.90								
01.Mai.90	120	120	1700	1892,215	1870,734	1935,467	1878,885	1897,918
01.Sep.90	243	200	1350	1369,151	1376,749	1350,976	1347,281	1349,102
01.Jän.91	365	300	1000	947,5046	946,9876	987,7405	1007,635	1027,928
01.Mai.91	485	400	800	699,9611	705,7844	744,3732	755,0244	784,3115
01.Sep.91	608	600	500	556,9848	559,7185	588,3601	596,0042	615,5926
01.Jän.92	730	800	380	464,9155	466,798	484,464	495,1324	504,2255
01.Mai.92	851	1000	300	395,1818	398,3709	414,974	424,5785	431,9068
01.Sep.92	974	1200	250	344,3671	345,3946	365,1153	373,0361	377,1487
01.Jän.93	1096	1400	230	305,5408	306,1023	326,1987	332,6153	337,1348
01.Mai.93	1216	1600	200	274,7425	275,3092	292,4118	301,8197	305,4063
01.Sep.93	1339	1800	180	249,1368	249,5756	265,9682	275,9781	279,5939
01.Jän.94	1461	2000	120	227,8559	228,3844	245,2395	253,7287	258,0176
01.Mai.94	1581			210,2465	210,8569	228,1901	234,804	240,0791
01.Sep.94	1704			194,8677	195,4409	213,3302	218,4389	223,9656
01.Jän.95	1826			181,7579	182,2105	200,6104	204,1587	209,8802
01.Mai.95	1946			170,4155	170,7616	189,616	191,608	197,2615
01.Jul.95	2007			164,9219	165,3583	184,48	185,7844	191,169

Figure 2-10: Comparison of WOPR for Well P3 at different Upscaling (Numerical model).
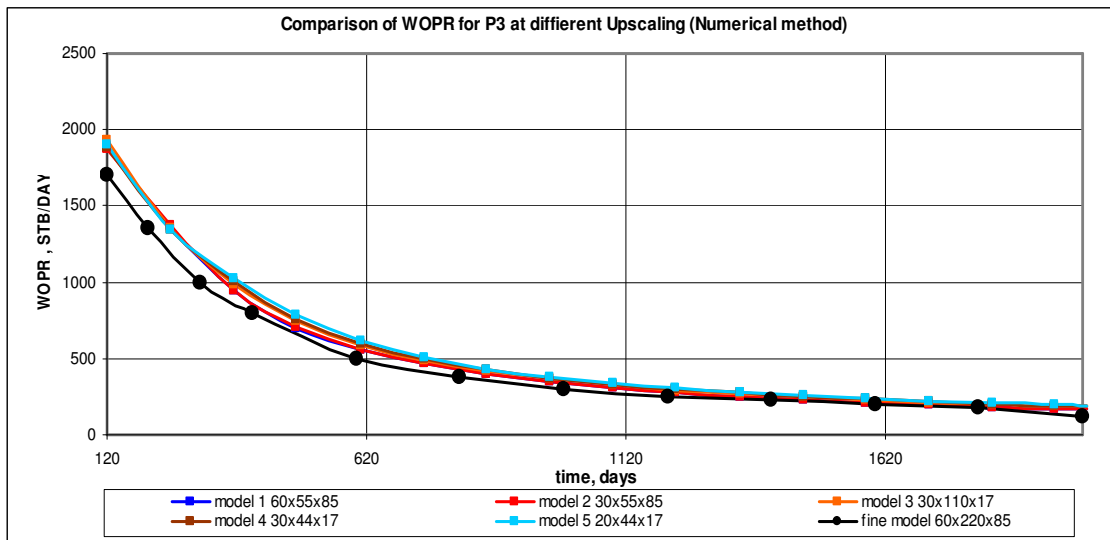
2.3.5 Comparison of Well Water Cut (WWCT) for P3 at Different Upscaling Models.

Analytical Method:

- Model 1 (60x55x85) and model 2 (30x55x85) was in a very good agreement with the fine model performance
- The three coarsest models model 3, model 4 and model 5 with dimensions of (30x110x17), (30x44x17) and (20x44x17) respectively underestimated the water cut for well P3 from the day 120. from those three models, model 3 was the closest then model 4 and model 5 respectively
- Model 3, model 4 and model 5 started with difference of 20 % form the fine model ,model 1 and model 2 , then in a gradual way the underestimation decreased to 10% after 700 days, and at the end of the period it was only 3% (Figure 2-11), (Table 2-14).

Numerical Method:

- At the beginning all the models underestimated the WWCT at different ratio and model 1 and model 2 were the closest to the fine model with 5% difference.
- All the models fitted the fine model after nearly 800 days, except model 5 which kept 5% difference until the end of the production period.
- All the models were acceptable cause of the small difference from the fine model at the end of production period (5% for model 5) (Figure 2-12), (Table 2-15).
- The original oil in place OOIP ,was the same in both method 10,772,610 STB

Table 2-14: Comparison of WWCT for Well P3 at different Upscaling (Analytical model).

Date	Days	Fine M. Days	Fine M. 60X220X85 WWCT P3 %	Model 1 60X55X85 WWCT P3 %	Model 2 30X55X85 WWCT P3 %	Model 3 30X110X17 WWCT P3 %	Model 4 30X44X17 WWCT P3 %	Model 5 20X44X17 WWCT P3 %
01.Jän.90			0	0	0	0	0	0
01.Mai.90	120	50	0	0,19855	0,186871	0,004769	0,002837	0,002519
01.Sep.90	243	100	0,2	0,489045	0,455373	0,252943	0,21171	0,173361
01.Jän.91	365	200	0,44	0,664442	0,644025	0,487638	0,462065	0,4401
01.Mai.91	485	300	0,6	0,750207	0,737721	0,634671	0,615482	0,592966
01.Sep.91	608	400	0,7	0,800375	0,791795	0,719629	0,705471	0,688179
01.Jän.92	730	600	0,8	0,833717	0,826672	0,773165	0,760684	0,748515
01.Mai.92	851	800	0,84	0,85747	0,850809	0,809378	0,79828	0,787675
01.Sep.92	974	1200	0,9	0,875444	0,869248	0,83641	0,826073	0,817216
01.Jän.93	1096	1600	0,92	0,889176	0,883636	0,856725	0,847154	0,839168
01.Mai.93	1216	2000	0,95	0,899896	0,895135	0,87232	0,86355	0,856514
01.Sep.93	1339			0,908814	0,904595	0,885087	0,877183	0,870713
01.Jän.94	1461			0,916125	0,912316	0,895373	0,888344	0,882467
01.Mai.94	1581			0,922171	0,918701	0,903784	0,897517	0,892059
01.Sep.94	1704			0,927458	0,924282	0,911071	0,905478	0,900491
01.Jän.95	1826			0,931987	0,929044	0,917239	0,912196	0,907576
01.Mai.95	1946			0,935899	0,933127	0,922515	0,917897	0,913518
01.Jul.95	2007			0,937716	0,935012	0,924937	0,920511	0,916278

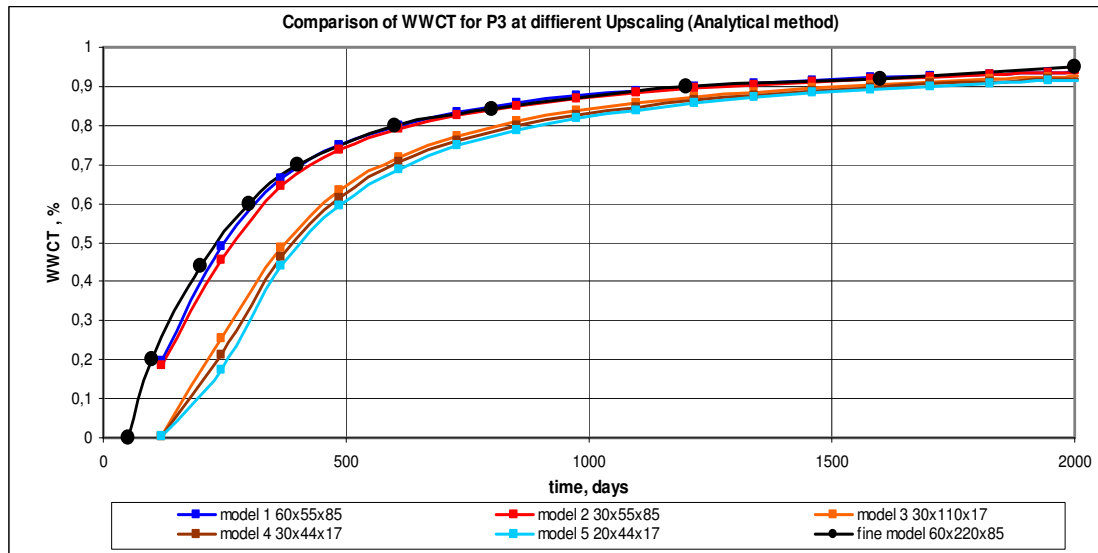**Figure 2-11: Comparison of WWCT for Well P3 at different Upscaling (Analytical model).**

Table 2-15: Comparison of WWCT for Well P3 at different Upscaling (Numerical model).

Date	Days	Fine M. Days	Fine M. 60X220X85 WWCT P3 %	Model 1 60X55X85 WWCT P3 %	Model 2 30X55X85 WWCT P3 %	Model 3 30X110X17 WWCT P3 %	Model 4 30X44X17 WWCT P3 %	Model 5 20X44X17 WWCT P3 %
01.Jän.90			0	0	0	0	0	0
01.Mai.90	120	50	0	0,169205	0,15117	0,092296	0,06493	0,042368
01.Sep.90	243	100	0,2	0,441381	0,419222	0,420427	0,376829	0,367738
01.Jän.91	365	200	0,44	0,623523	0,609778	0,585671	0,542358	0,525164
01.Mai.91	485	300	0,6	0,724199	0,710923	0,689782	0,658722	0,639146
01.Sep.91	608	400	0,7	0,780976	0,771399	0,756102	0,731873	0,718139
01.Jän.92	730	600	0,8	0,817351	0,809487	0,799828	0,778076	0,769852
01.Mai.92	851	800	0,84	0,844847	0,83752	0,829077	0,810147	0,803249
01.Sep.92	974	1200	0,9	0,864729	0,859131	0,849846	0,833398	0,828424
01.Jän.93	1096	1600	0,92	0,879848	0,875089	0,865763	0,8515	0,846702
01.Mai.93	1216	2000	0,95	0,891812	0,887547	0,879513	0,865223	0,861085
01.Sep.93	1339			0,901768	0,897926	0,890263	0,876714	0,872787
01.Jän.94	1461			0,910035	0,906478	0,89866	0,886589	0,882561
01.Mai.94	1581			0,916867	0,913543	0,905541	0,894995	0,890672
01.Sep.94	1704			0,922824	0,919753	0,911512	0,902249	0,897935
01.Jän.95	1826			0,927896	0,925076	0,916629	0,908562	0,904284
01.Mai.95	1946			0,93228	0,929681	0,92106	0,914116	0,909944
01.Jul.95	2007			0,934405	0,931854	0,923136	0,916693	0,912678

Figure 2-12: Comparison of WWCT for Well P3 at different Upscaling (Numerical model).
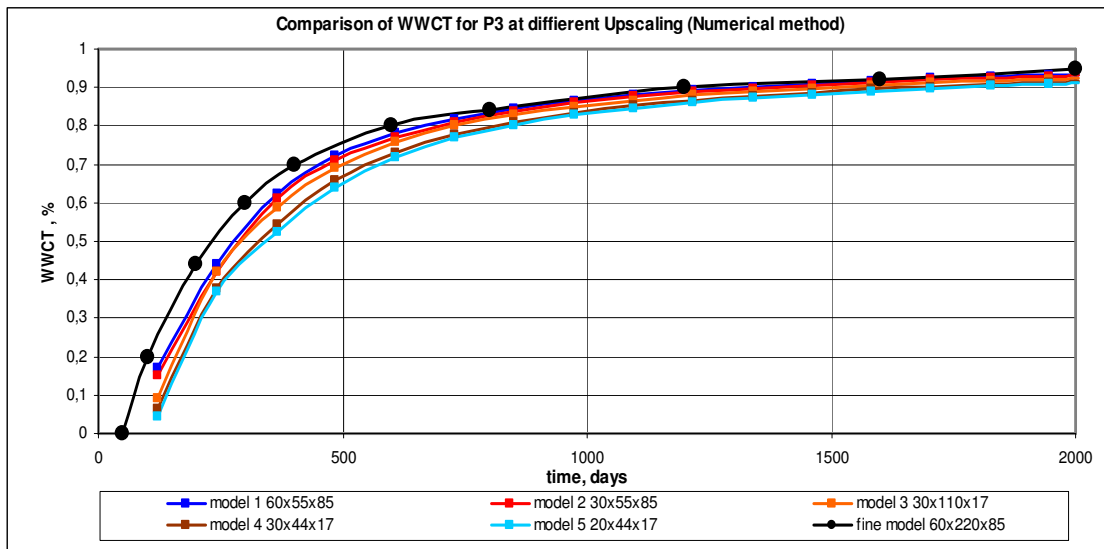
2.3.6 Comparison of Field Reservoir Pressure (FPR) at Different Upscaling Models.

Analytical Method:

- There was about 500 psi different at the start point between all the models and the fine model.

- All the models showed sharp pressure drop until 120 days ,for instant model 1 is the closest model to the fine model that have got pressure drop from 6000 psi to 4676, after that the pressure start to drop gradually.

- All the models were behaving the same, although they were not identical.

- Model 1 was the nearest model to the fine model then model 2,model 3, model 4 and model 5 respectively.

- At the end of the production period the pressure remain 4500 psi for the fine model and for model 1 was 4290 psi (closest model to the fine model) (Figure 2-13), (Table 2-16).

Numerical Method:

- There was about 500 psi different at the start point between all the models and the fine model.

- All the models showed dramatically pressure drop until 120 days, after that the pressure start to drop gradually, and the sudden pressure drop was 1000 psi.

- The loss of accuracy between the fine model and the other models started to decrease with time until 1200 day after that it remain constant with different of about 100 psi.

- All the models were behaving the same with slight difference in the values.

- Model 1 was the nearest model to the fine model then model 2, model 3, model 4 and model 5 respectively.

- At the end of the production period the pressure remain 4500 psi for the fine model and for model 1 was 4404 psi (closest model to the fine model) (Figure 2-14), (Table 2-17).

- The original oil in place OOIP ,was the same in both method 10,772,610 STB

Table 2-16: Comparison of FPR at different Upscaling (Analytical model).

Date	Days	Fine M. Days	Fine M. 60X220X85 FPR Field PSI	Model 1 60X55X85 FPR Field PSI	Model 2 30X55X85 FPR Field PSI	Model 3 30X110X17 FPR Field PSI	Model 4 30X44X17 FPR Field PSI	Model 5 20X44X17 FPR Field PSI
01.Jän.90	0	0	5580	6029,733	6029,733	6029,718	6029,718	6029,718
01.Mai.90	120	50	5500	4676,37	4519,681	4287,051	4207,639	4178,136
01.Sep.90	243	100	5490	4599,677	4463,948	4275,636	4203,103	4174,743
01.Jän.91	365	200	5350	4513,601	4394,952	4249,643	4186,262	4160,718
01.Mai.91	485	400	5100	4450,768	4347,743	4224,268	4166,041	4144,169
01.Sep.91	608	600	4900	4407,328	4314,055	4202,482	4150,134	4130,875
01.Jän.92	730	800	4750	4375,613	4289,997	4185,926	4138,658	4120,832
01.Mai.92	851	1000	4650	4351,671	4271,85	4173,203	4129,711	4113,323
01.Sep.92	974	1200	4600	4332,363	4257,238	4162,817	4122,431	4107,177
01.Jän.93	1096	1400	4550	4316,646	4245,433	4154,356	4116,407	4102,161
01.Mai.93	1216	1600	4520	4303,749	4235,658	4147,513	4111,549	4098,063
01.Sep.93	1339	1800	4510	4292,517	4227,113	4141,623	4107,358	4094,516
01.Jän.94	1461	2000	4500	4282,896	4219,846	4136,64	4103,796	4091,486
01.Mai.94	1581			4274,58	4213,599	4132,393	4100,752	4088,905
01.Sep.94	1704			4267,003	4207,922	4128,548	4098,015	4086,593
01.Jän.95	1826			4260,267	4202,913	4125,175	4095,632	4084,574
01.Mai.95	1946			4254,308	4198,465	4122,205	4093,55	4082,828
01.Jul.95	2007			4251,501	4196,368	4120,817	4092,58	4082,029

Figure 2-13: Comparison of FPR at different Upscaling (Analytical model).
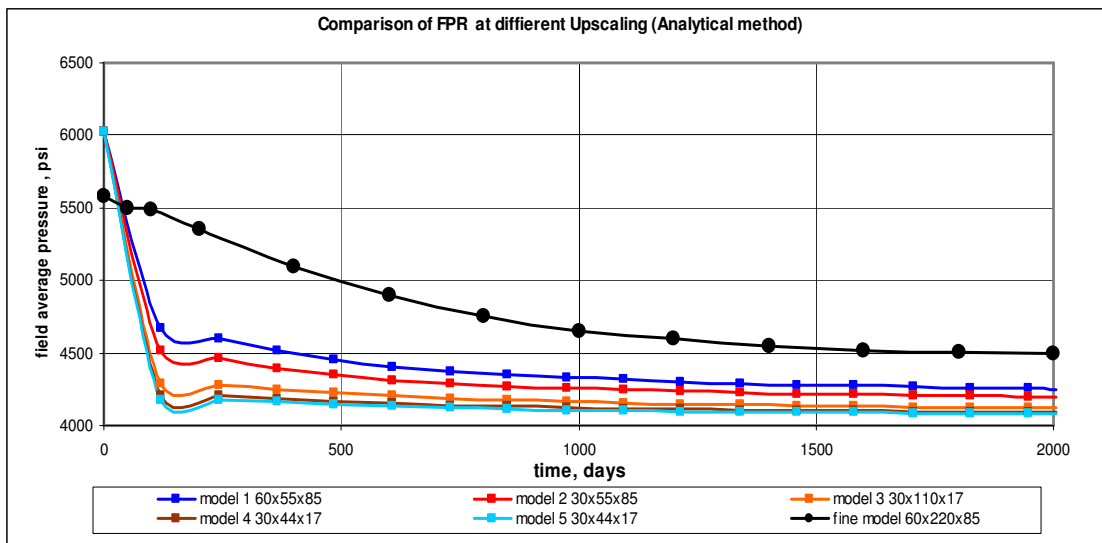
Table 2-17: Comparison of FPR at different Upscaling (Numerical model).

Date	Days	Fine M. Days	Fine M. 60X220X85 FPR Field PSI	Model 1 60X55X85 FPR Field PSI	Model 2 30X55X85 FPR Field PSI	Model 3 30X110X17 FPR Field PSI	Model 4 30X44X17 FPR Field PSI	Model 5 20X44X17 FPR Field PSI
01.Jän.90	0	0	5580	6029,733	6029,733	6029,718	6029,718	6029,718
01.Mai.90	120	50	5500	5087,008	5030,405	4985,743	4954,462	4918,475
01.Sep.90	243	100	5490	4963,76	4916,587	4855,328	4830,623	4802,378
01.Jän.91	365	200	5350	4829,544	4786,827	4736,181	4718,052	4698,516
01.Mai.91	485	400	5100	4728,739	4692,907	4650,83	4635,187	4620,053
01.Sep.91	608	600	4900	4656,196	4624,248	4588,201	4572,931	4560,388
01.Jän.92	730	800	4750	4604,52	4574,71	4543,428	4528,783	4514,939
01.Mai.92	851	1000	4650	4565,134	4537,262	4509,229	4493,952	4481,538
01.Sep.92	974	1200	4600	4533,111	4506,755	4481,824	4466,528	4454,211
01.Jän.93	1096	1400	4550	4507,152	4482,283	4459,357	4444,046	4432,768
01.Mai.93	1216	1600	4520	4485,806	4462,11	4440,974	4425,833	4414,731
01.Sep.93	1339	1800	4510	4467,235	4444,493	4425,078	4409,695	4399,181
01.Jän.94	1461	2000	4500	4451,36	4429,448	4411,56	4396,075	4385,773
01.Mai.94	1581			4437,671	4416,49	4399,797	4384,395	4374,35
01.Sep.94	1704			4425,22	4404,711	4389,071	4373,932	4363,949
01.Jän.95	1826			4414,199	4394,272	4379,594	4364,587	4354,923
01.Mai.95	1946			4404,459	4385,04	4371,27	4356,398	4346,943
01.Jul.95	2007			4399,865	4380,684	4367,365	4352,532	4343,107

Figure 2-14: Comparison of FPR at different Upscaling (Numerical model)
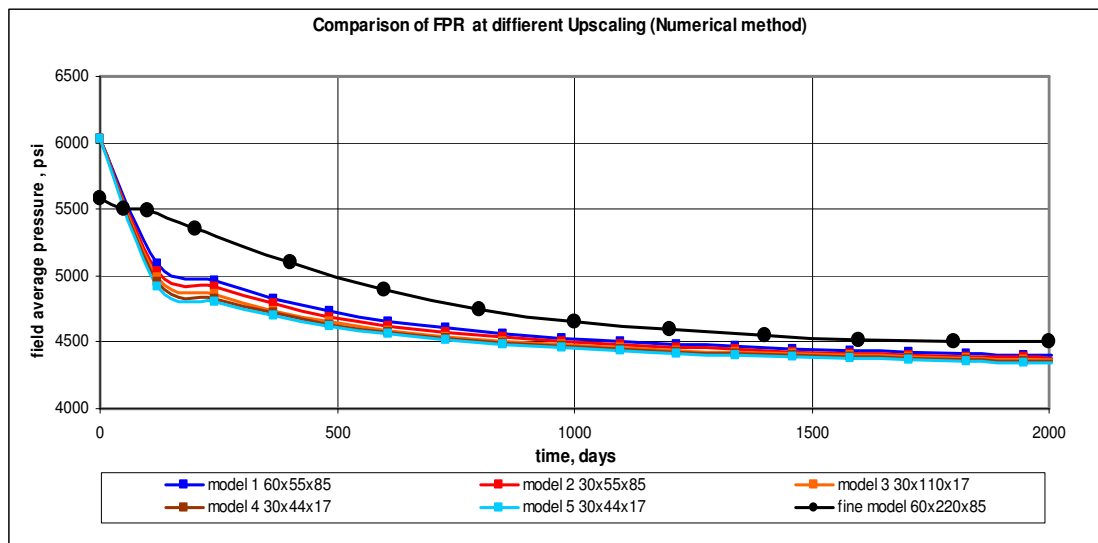
2.3.7 Comparison between the CPU time between the Analytical and Numerical approach.

- The CPU time for the analytical method was less than the CPU time for the numerical method for the coarsened models 3, 4, 5 respectively.
- The CPU time for the analytical method increased gradually with number of cells.
- The CPU time for the numerical method increased dramatically for the large models 1, 2 respectively (Figure 2-15), (Table 2-18).

Table 2-18: Comparison of CPU time for Analytical and Numerical models.

Models	Cells in			Total Cells	CPU time (Ana.)		CPU time (Num.)	
	I	J	K		Second	day	Second	day
fine model	60	220	85	1.122.000				
model 0	60	110	85	561.000		> 7 days		
model 1	60	55	85	280.500	172800	2	61568	0,712593
model 2	30	55	85	140.250	38959	0,4509144	19483	0,225498
model 3	30	110	17	56.100	854	0,0098843	4782	0,055347
model 4	30	44	17	22.440	50	0,0005787	506	0,005856
model 5	20	44	17	14.960	25	0,0002894	220	0,002546

Figure 2-15: Comparison of CPU time for Analytical and Numerical models.
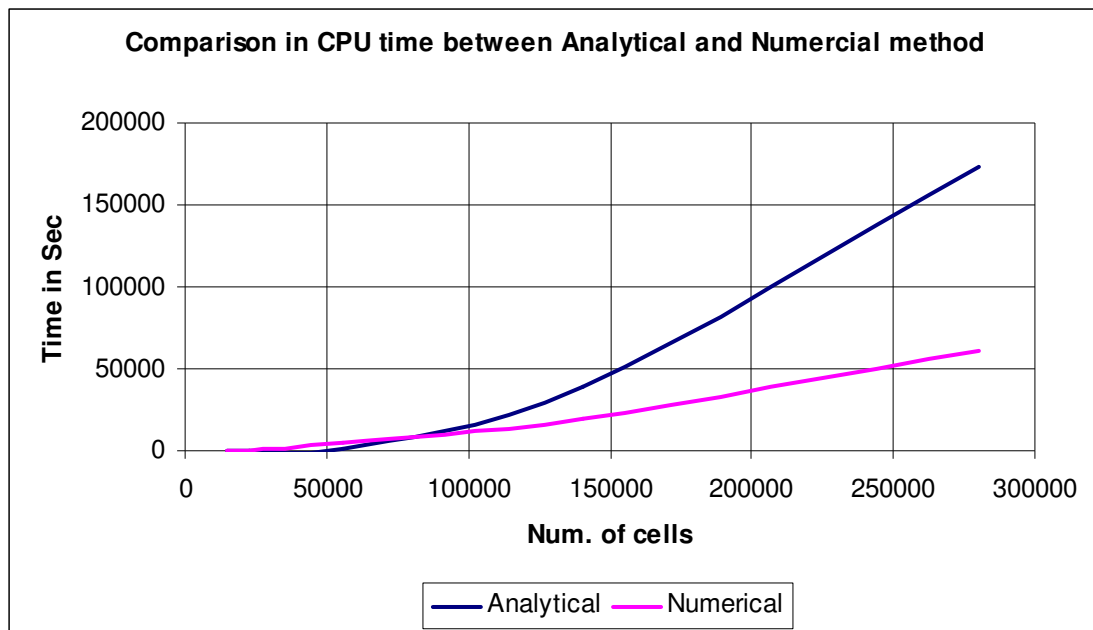
2.3.8 Comparison between some models in 2D and 3D scaling view in Petrel^{TM} at different scales.

The comparison in the 2-D and 3-D upscaling view will be between model 2 (30x55x85), model5 (20x44x17) and the fine model (60x220x85).

## 2.3.8.1 Top View 2D for the First Layer.

Permeability in X Direction in 2D

Fine Model (60x110x85) and Model 2 (30x55x85)
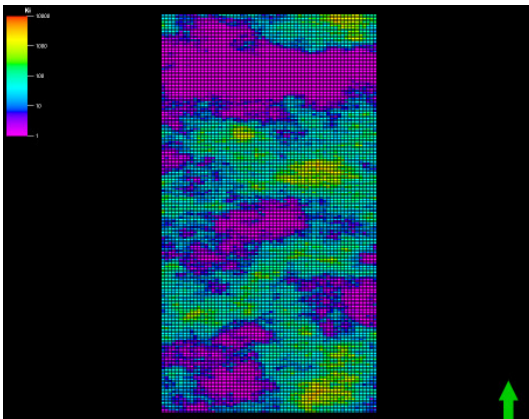
- Fine Model (60x110x85)

Model 2 (30x55x85)
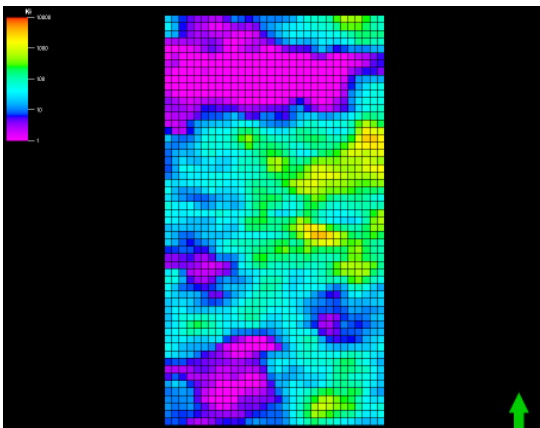
Numerical method   Analytical method
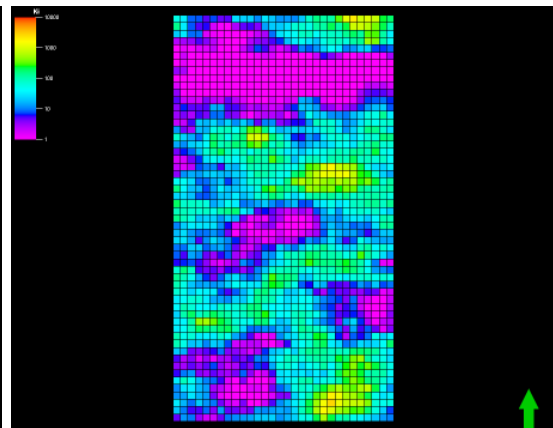
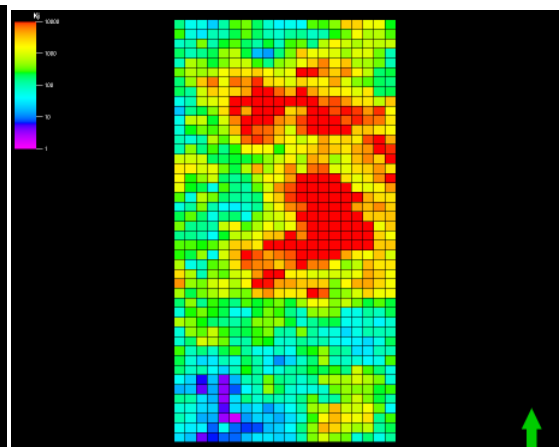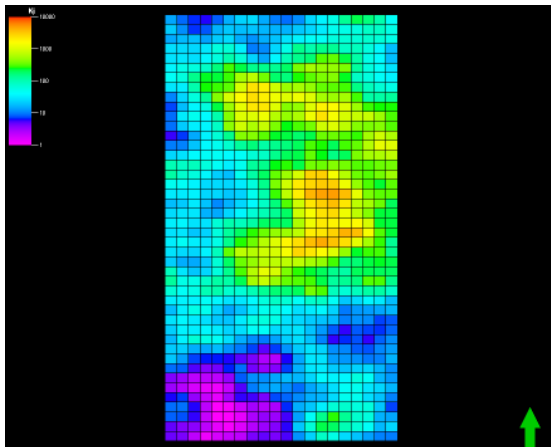## Fine Model (60x110x85) and Model 5 (20x44x17)

- Fine Model (60x110x85)
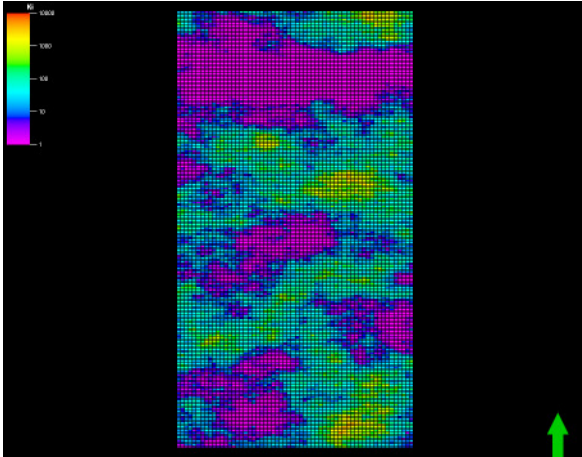
Model 5 (20x44x17)
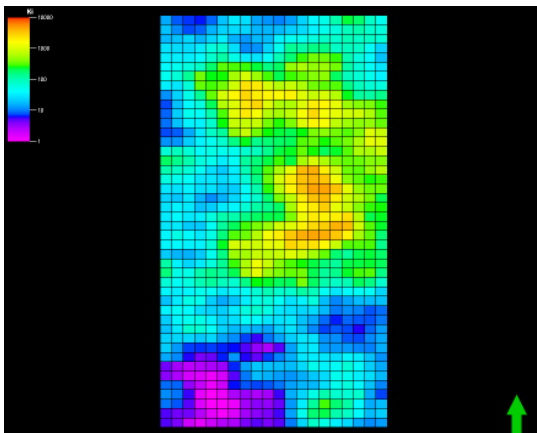
Numerical method	Analytical method
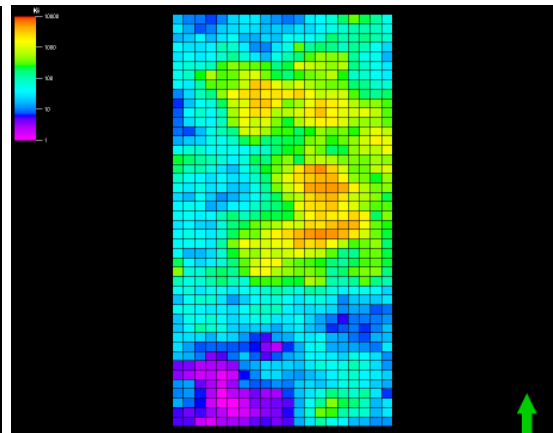
Observation of Permeability in X Direction in 2D

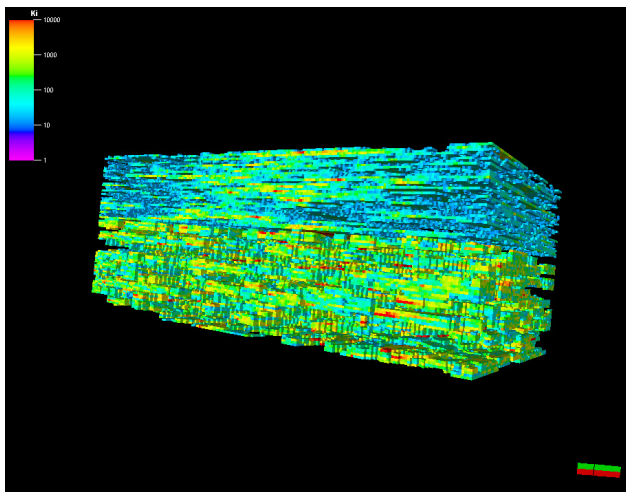The result of upscaling in X direction from normal visualization indicated the following:

- The analytical method showed a closer distribution of the permeability in X direction than the numerical method.

- In the numerical method most of the low values of the permeability in X direction in the right middle of the map has disappeared, although the map still showing good distribution.

Permeability in Y Direction in 2D
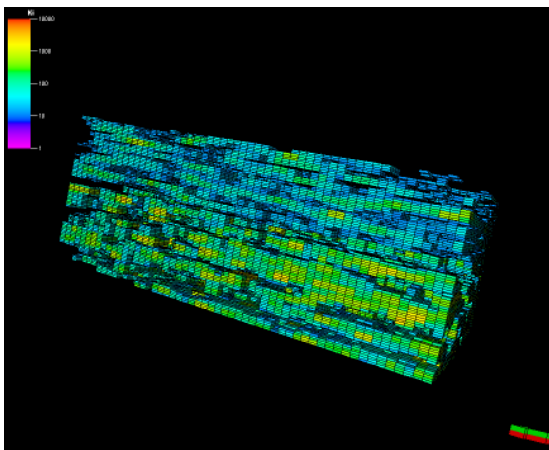
Fine Model (60x110x85) and Model 2 (30x55x85)
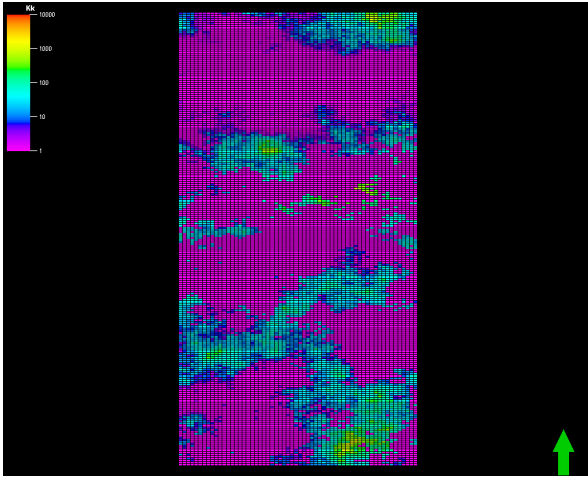
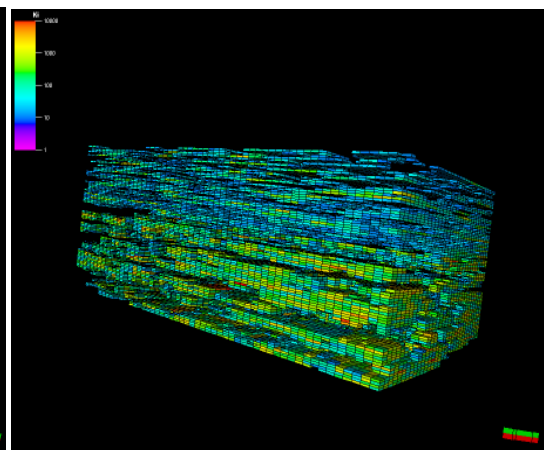- Fine Model (60x110x85)

- Model 2 (30x55x85)
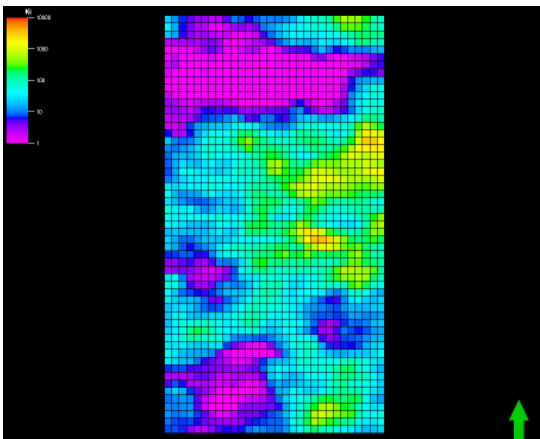
Numerical method   Analytical method
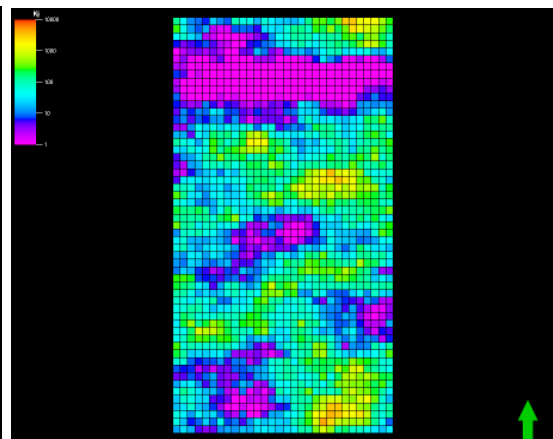
Fine Model (60x110x85) and Model 5 (20x44x17)

- Fine Model (60x110x85)
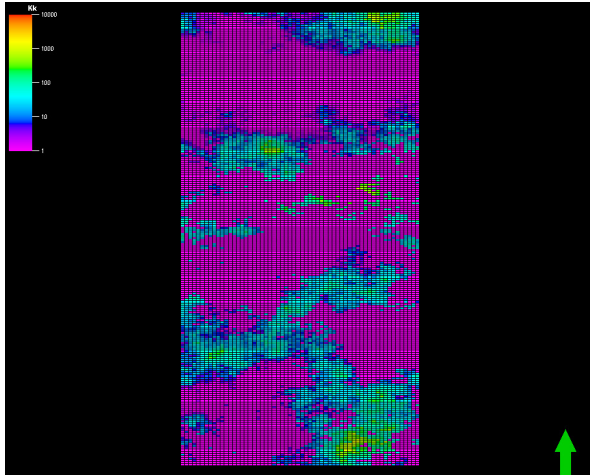
- Model 5 20x44x17

Numerical method   Analytical method

Observation of Permeability in Y Direction in 2D

The result of upscaling in Y direction from normal visualization indicated the following:

- The analytical method showed a high values distribution of the permeability in Y direction than the numerical method, and it was totally far from the fine model.

- In the numerical method, at the bottom left corner of the map, the features were a bit close to the fine model.

- None of the methods showed a good agreement with the fine model.

- The two methods were close to each other than to the fine model.

2.3.9 Three Dimension View (3D).

Permeability in X Direction in 3D

Fine Model (60x110x85) and Model 2 (30x55x85)

- Fine Model (60x110x85)

- Model 2 (30x55x85)

Numerical method   Analytical method
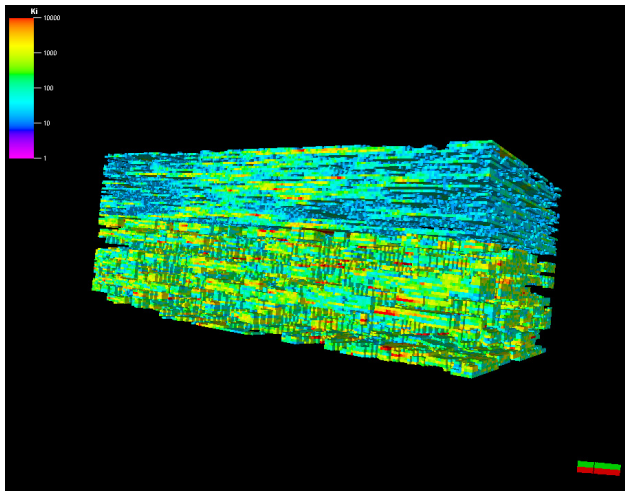
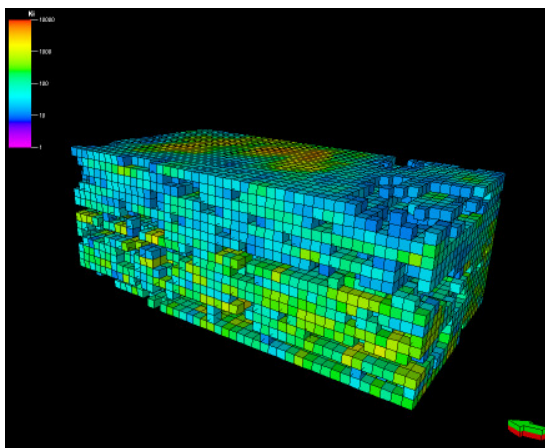**Fine Model (60x110x85) and Model 5 (20x44x17)**

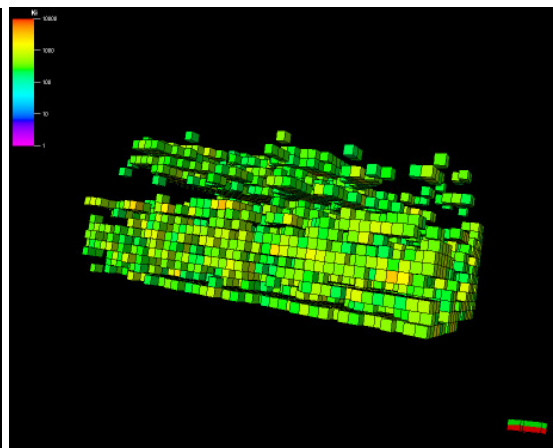- Fine Model (60x110x85)

- Model 5 20x44x17

Numerical method   Analytical method

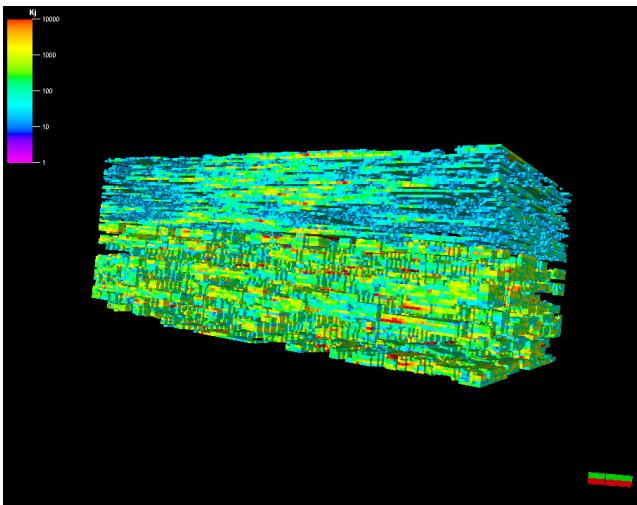## Observation of Permeability in X Direction in 3D

The result of upscaling for the permeability in X direction from normal visualization indicated the following:

- The gaps in the models represent all the values of permeability less than 10 mD.

- The analytical method for model 2 showed a good agreement to the final model over all field view.

- In the numerical method showed a good agreement as well to the final model over all field view.

- The numerical method represents most likely the same permeability distribution of the fine model.
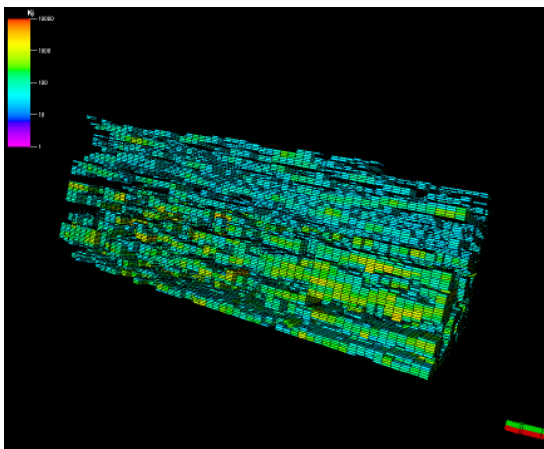
Permeability in Y direction in 3D

Fine Model (60x110x85) and Model 2 (30x55x85)

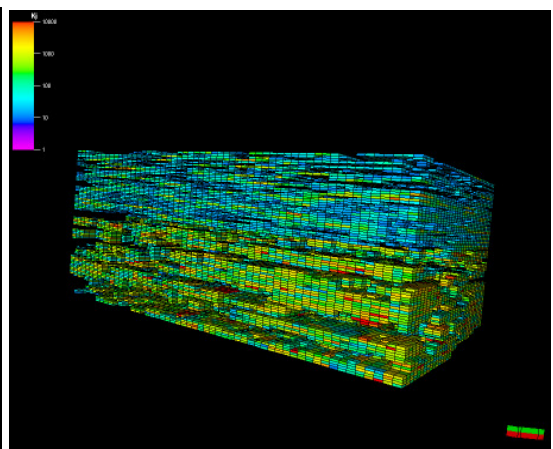- Fine Model (60x110x85)

- Model 2 (30x55x85)

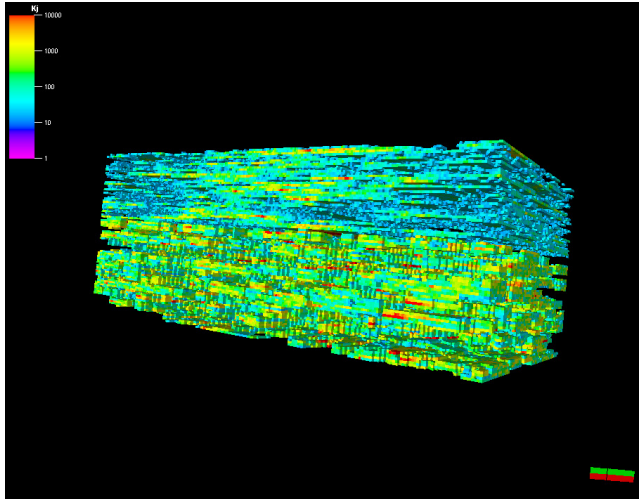Numerical method   Analytical method

Fine Model (60x110x85) and Model 5 (20x44x17)

- Fine Model (60x110x85)

- Model 5 20x44x17
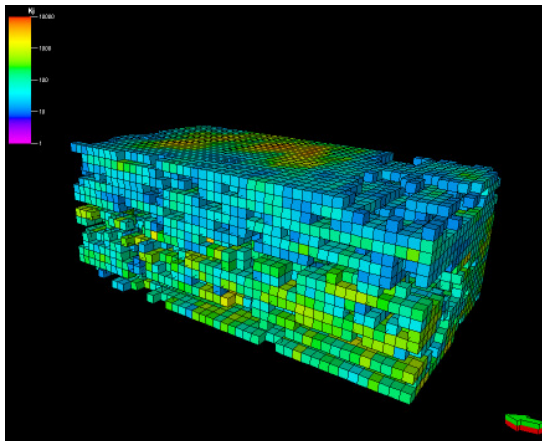
Numerical method   Analytical method

Observation of Permeability in Y Direction in 3D

The result of upscaling for the permeability in Y direction from normal visualization indicated the following:

- The gaps in the models represent all the values of permeability less than 10 mD.

- The analytical method for model 2 gave a better representation of the fine model

- The analytical method for model 5 did not give good representation to the fine model.

- The numerical method for model 2 showed a good agreement but not as the analytical method did.

- The numerical method for model 5 showed a good agreement to the final model over all field view.

- The numerical method for model 5 represents most likely the same permeability distribution of the fine model.

Permeability in Z Direction in 3D

Fine Model (60x110x85) and Model 2 (30x55x85)

- Fine Model (60x110x85)

- Model 2 (30x55x85)

Numerical method   Analytical method
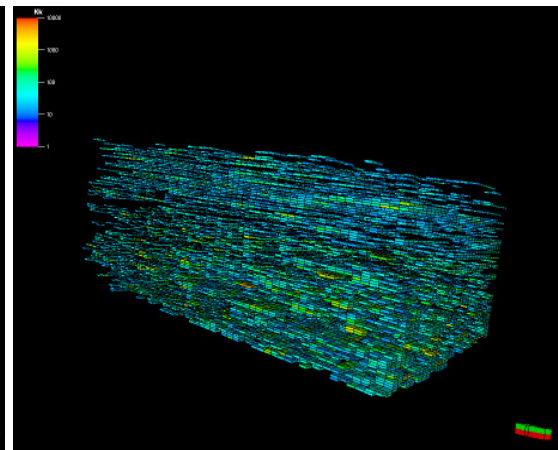
Fine Model (60x110x85) and Model 5 (20x44x17)
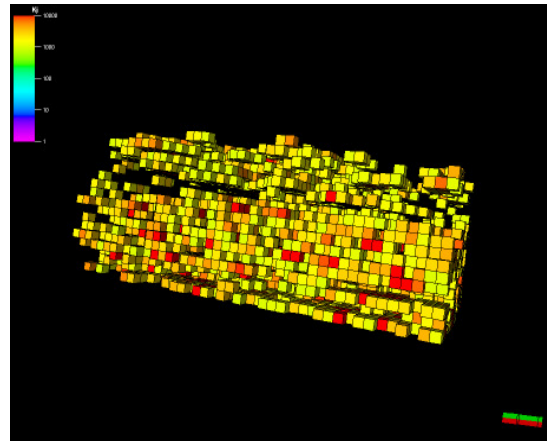
- Fine Model (60x110x85)
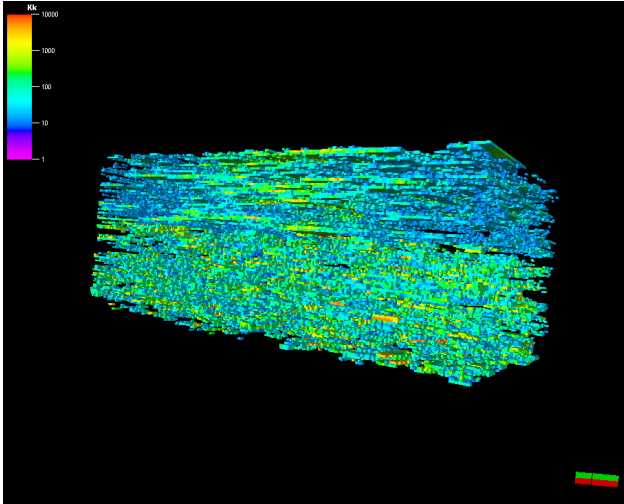
- Model 5 20x44x17
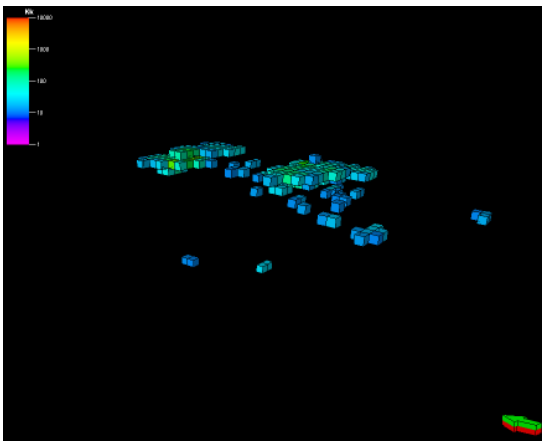
Numerical method   Analytical method

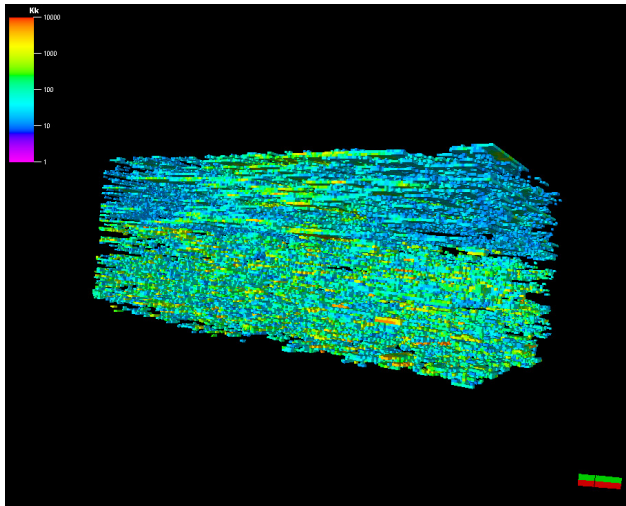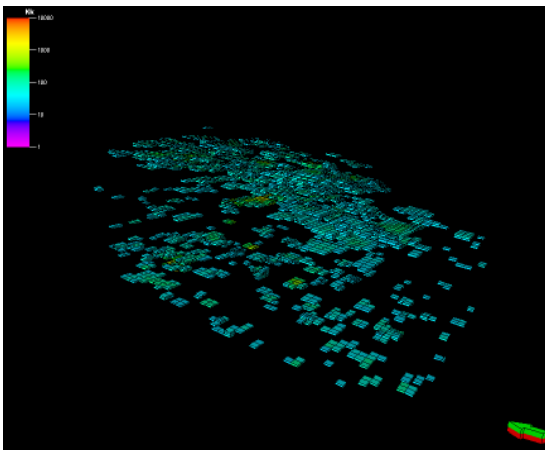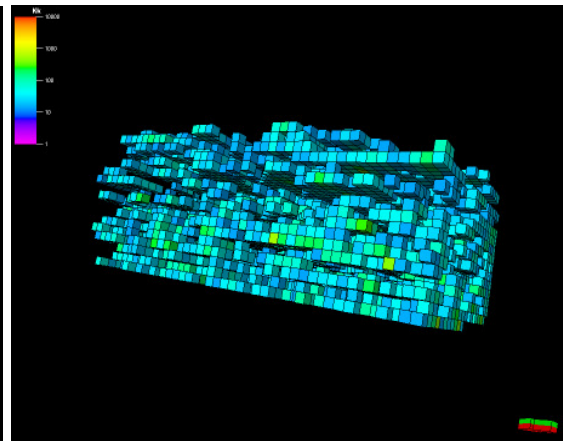## Observation of Permeability in Z Direction in 3D

The result of upscaling for the permeability in Z direction from normal visualization indicated the following:

- The gaps in the models represent all the values of permeability less than 10 mD.

- The analytical method for model 2 gave a better representation of the fine model

- The analytical method for model 5 gave a good representation to the fine model as the model 2 did.

- The numerical method for model 2 showed a poor representation if we compare it to the fine model.

- The numerical method for model 5 showed a very poor distribution permeability comparing it with the fine model and with the analytical method for the same model.

Chapter 3

3 Conclusions

Through all of my research, the following conclusions can be drawn:

1- The 10th SPE comparative solution project was used in this thesis as the fine model to perform upgridding and upscaling, this model has a simple geometry with 1.122×10^6 cells.
   The Petrel^{TM} (schlumberger package) was used to perform upscaling to the properties (permeability and porosity) on five geometrical models. The five models were created in Petrel^{TM} for this purpose (coarse models), and exported to the dynamic simulator (Eclipse).
   The dynamic scenario was assumed to inject water at the center of the models (injector well) with injection rate 5000 bbl/day in all layers and to produce fluid from four producers located at the four corners of the model with bottom hole pressure 4000 psi. The dynamic simulation was done for 2000 day with time step each 3 month.

2- The quality of the upscaling did not depend on the upscaling of the structure only but also on the method by which the properties such as permeability were upscaled. In this research analytical and numerical averaging were used to upscale the permeability; however, if any other averaging method was used the results would have deviated, sometimes, significantly.

3- The macroscopic behavior is affected by the small-scale transport even when a very heterogeneous field-scale reservoir description is used. The heterogeneity in Z direction (vertical) is much larger than the heterogeneity in X and Y direction (horizontal) and for that reason the Upscaling in Z direction has the significant effect on the dynamic simulation result.

4- Since upscaling had significant impact on dynamic behavior of the coarse models, the coarsened model could be achieved faster (simulation run time). More than five

models were created at the beginning and were excluded later on from the results due to the time consuming i.e., 561.000 cells took 5 days to complete a run for 2000 day.

5- The comparison between the two approach averaging methods was obviously clear that the numerical method by using diagonal tensor method gave a better result than the analytical method did. Flow-based upscaling is a more sophisticated method designed specifically for permeability. It involves performing a flow simulation on the block of fine cells coinciding with each coarse cell to determine a representative coarse cell permeability value. The tensor upscaling process will calculate I, J, and K permeabilities from input as permeability in the I, J and K directions and porosity.

6- For additive rock properties, such as porosity and saturation, a simple averaging algorithm such as the 'volume weighted arithmetic average' could be considered as the best estimator in determining the effective porosity of the coarser grid.

7- Since some of the 3D view showed that the numerical approach gave results near to the fine model and in another time analytical approach gave the nearest results to the fine model than the numerical did, for that reason the judgment from the normal visualization of the 3D grid block is not a good indicator for the upscaling performance. So running the simulation is kept the right way to consider the result as close or far from the fine model.

8- Finally, it is very important that we achieve a better understanding of the error introduced by the various upscaling procedures. By quantifying this error through the development of error models, we will be able to determine the appropriate upscaling method and level of coarsening to use for a particular problem.

Chapter 4

4   References

[1]   Sameer A.Khan and Aaron G.Dawson.: ``Method of Upscaling Permeability for unstructured grids,'' United State Patent Issued on, November 30, 2004.

[2]   Petrel[TM] 2007.1 Reference Manual, Schlumberger, (2007).

[3]   A. Kumer, SPE, and C. L Farmer, SPE, Schlumberger GeoQuest, G. R. Jerauld, SPE, ARCO Exploration and Production Technology, and D. Li, SPE, Mobil E&P Technical Center.: "Efficient Upscaling from Coarse to Simulation Models," paper SPE 38744 presented at the 1997 SPE Annual Technical Conference and Exhibition held in San Antonio, Taxes, 5-8 October 1997.

[4]   Chawathe,A., and Taggart, I.: "Insight into Upscaling Using 3D Streamline," paper SPE 88846 published in 2004. Revised publication from paper SPE 66379 presented at the 2001 SPE Reservoir Simulation Symposium, Houston, 11-14 February.

[5]   Luca Consentino.: "Integrated Reservoir study," Book – Technology (2001).

[6]   Stefan M. Luthi.: "Geological well logs their use in Reservoir Modeling," Book- Technology (2001).

[7]   Mike Carlson.: "Practical Reservoir Simulation," Book – Technology (2003).

[8]   Hartanto Lina. 2004. Different scales and integration of data in reservoir simulation. PhD Thesis, Curtin University of Technology.

[9]   Dongxiao Zhang.: "Stochastic Methods for Flow in Porous Media," Copying with Uncertainties.

[10]   J.A. Lozano, L.P. Costa. F.B. Alves & A.C Silva. Partex-CPS, Portugal: "Upscaling of Stochastic Model for Reservoir Simulation – An Integrated Approach," paper SPE 36205 This paper was prepared for presentation at the 7th Abu Dhabi International Petroleum Exhibition and Conference held In Abu Dhabi, U.A.E., 13.16 October 1996.

[11]   Yi-Kun Yang, SPE M.D. Deo, SPE, University of Utah.: "Full-Tensor Multiphase Flow Simulations With Applications to Upscaling and Discrete-Fracture Models," paper SPE 66348. This paper was prepared for presentation

at the SPE Reservoir Simulation Symposium held in Houston, Texas, 11–14 February 2001.

[12]   S.S. Guedes, SPE, Petrobrás, and D.J. Schiozer, SPE, U. of Campinas.: "An Implicit Treatment of Upscaling in Numerical Reservoir Simulation,"

[13]   S Gillian Pickup, SPE, Heriot-Watt U.; P.S. Ringrose, SPE, Statoil; and Ahmed Sharif, Roxar.: "Steady-State Upscaling: From Lamina-Scale to Full-Field Model,"

[14]   M A Christie, SPE, Heriot-watt University, and M J Blunt, SPE, Imperial College.: " Tenth SPE Comparative Solution Project: A Comparison of Upscaling Techniques" paper SPE 66599. This paper was prepared for presentation at the SPE Reservoir Simulation Symposium held in Houston, Texas, 11–14 February 2001.

[15]   Web Site for 10th SPE Comparative Solution Project: http://www.spe.org/csp/

[16]   Christie et al., "Tenth SPE Comparative Solution Project: A Comparison of Upscaling Techniques" paper SPE 72469. 2001, p. 308-316.

Appendix A

Derivation of Some Existing Algorithms

- **Darcy's law**

The equation which governs most upscaling algorithms' principal is the basic fluid flow equation in the porous media known as Darcy's law. Darcy's law states that the fluid flow rate is proportional to the cross sectional area and the pressure difference ΔP (Pb-Pa) across a length of Δx, and inversely proportional to the viscosity of the fluid. The proportional constant is referred to as the 'permeability. Therefore, for a single phase flow in horizontal direction, it is defined as:

$$q = \frac{k_x A}{\mu} \frac{\Delta P}{\Delta x} \qquad \text{(A-1)}$$
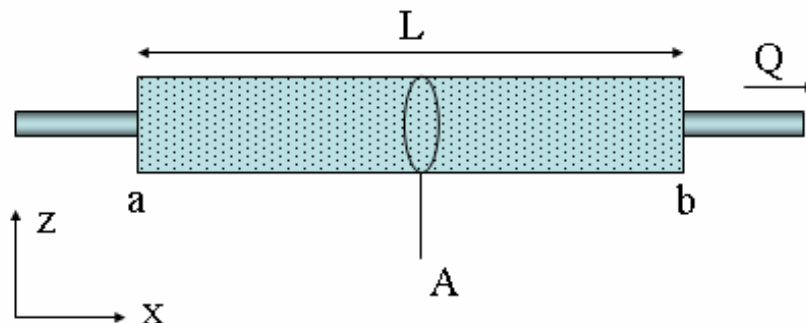
Darcy's law

Figure A-1 Graphical representation of Darcy's law

Permeability is a physical property of a large number of pores which influence the tendency of the fluid to flow from one place to another. The permeability usually decrease as the as the grain size decreases. This is normally used to distinguish the rock type classification depending upon its geological rock depositional and its properties. For example, the clean and unconsolidated sand may have a permeability as high as 5 to 10 Darcies, while the compacted and cemented sandstone rocks tend to have lower permeability. Productive sandstone reservoirs usually have permeability in the range of 10 to 1000 mD. Furthermore, the presence of clay, which may swell on contact with fresh water, can also affect permeability resulting in the reduction of rock's permeability by several orders of magnitude.

Permeability does not act upon one direction. The flow in porous media often occur in three principle directions, horizontally on x and y directions and also vertically on the z direction. Therefore, by regarding the potential gravitational effects, the three directional flows can be defined as:

$$\begin{bmatrix} Q_x \\ Q_y \\ Q_z \end{bmatrix} = - \frac{A}{\mu} \begin{bmatrix} K_{xx} & K_{xy} & K_{xz} \\ K_{yx} & K_{yy} & K_{yz} \\ K_{zx} & K_{zy} & K_{zz} \end{bmatrix} \begin{bmatrix} \partial\phi/\partial x \\ \partial\phi/\partial y \\ \partial\phi/\partial z \end{bmatrix} \qquad (A\text{-}2)$$

Darcy's law in 3-D flow

• **Effective Reservoir Properties**

In the reservoir modelling, the reservoir properties, which include porosity, permeability and fluid saturation, are typically assigned with the average value representation on each individual grid cells. The average cell value is normally called 'the effective property' of a heterogeneous block.
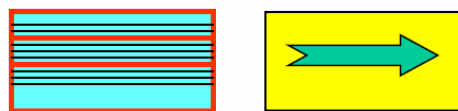
Figure A-2 Graphical representation of effective properties

• **Porosity and Initial Fluid Saturation**

For the porosity or the initial fluid saturation, the effective properties can easily be defined as these properties serve a function of preserving the total pore volume and the pore volume occupied by the fluid for the porosity and water saturation respectively.

By definition, the pore volume is basically the combination of the grid block porosity with the volume of the block, while the fluid pore volume is the combination of pore volume and the percentage of fluid saturation within the pore volume.

Porosity

The definition of the effective porosity can then be derived with the following equations.

Pore volume at coarse scale = total pore volume at fine scale

$$PV_{coarse} = \sum PV_{i, \, fine} \tag{A-3}$$

$$V_{bulk, \, coarse} \cdot \bar{\phi} = \sum V_{bulk, \, i, \, fine} \cdot \phi_{i, \, fine} \tag{A-4}$$

$$\bar{\phi} = \frac{\sum V_{bulk, \, i, \, fine} \cdot \phi_{i, \, fine}}{V_{bulk, \, coarse}} \tag{A-5}$$

Derivation of effective porosity

Therefore, from the derivation shown above, the effective porosity can be defined by using the bulk volume weighted arithmetic average.

Initial Fluid Saturation

Similar to porosity, the initial fluid saturation will effect the total pore volume occupied by the fluid with in the medium. In the reservoir modelling, the initial fluid saturation is normally assigned by using the water saturation, while the remaining pore volume will be the pore volume occupied by the hydrocarbon. As mentioned earlier, preserving the hydrocarbon pore volume between the two different scales will be the main objective in creating the effective fluid saturation.

$$HCPV_{coarse} = \sum HCPV_{i, \, fine} \tag{A-6}$$

$$V_{bulk, \, coarse} \cdot \bar{\phi} \, (1 - \bar{S}_w) = \sum V_{bulk, \, i, \, fine} \cdot \phi_{i, \, fine} \cdot (1 - S_w) \tag{A-7}$$

$$PV_{coarse} \cdot (1 - \bar{S}_w) = \sum PV_{i, \, fine} \cdot (1 - S_w) \tag{A-8}$$

$$(1 - \bar{S}_w) = \frac{\sum PV_{bulk, \, i, \, fine} \cdot (1 - S_{w,i})}{PV_{coarse}} \tag{A-9}$$

$$\overline{S}_w = 1 - \frac{\sum PV_{bulk, i, fine} \cdot (1 - S_{w,i})}{PV_{coarse}} \qquad (A\text{-}10)$$

The above equations is the derivation of effective initial water saturation

From the derivation shown above, the effective water saturation can be defined by using the pore volume weighted arithmetic average.

- **Permeability**

For the permeability, which depends on the boundary conditions, the derivation is not as straight forward as the effective porosity or effective initial water saturation. The effective permeability is defined as the permeability of the homogeneous block, which will produce the same fluid flow under the same boundary conditions. The effective permeability is influenced by the boundary conditions, the geological depositional bedding and also the fluid flow within the system.

Therefore, for simplicity, here are the following two derivations for determining the upper and lower bounds of the effective permeability by using the arithmetic and harmonic upscaling algorithms respectively.

- **Arithmetic Upscaling Algorithm Derived based on Parallel Bed (Liner Flow)**

The arithmetic algorithm uses the assumption that the fluid flow in the linear manner, which can be described as the fluid flow in the parallel bed having a different permeability for each layer.
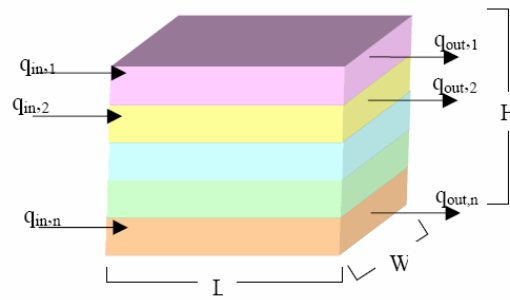
Fine Scale
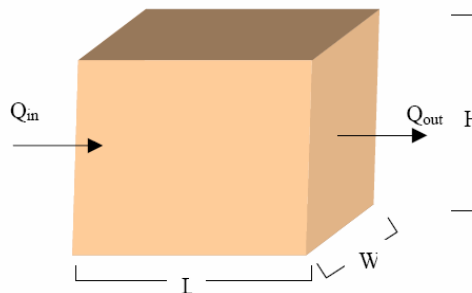
Coarse Scale

Figure A-3 Graphical representation of linear Flow in parallel bed for arithmetic upscaling algorithm derivation

For a fluid flow in the same boundary conditions, the pressure is assumed to be constant at each end of the flow system. The total flow rate can then be represented as the sum of the rates q_i in each layer.

$$Q_T = \sum_i q_i \tag{A-11}$$

By applying Darcy's law of equation can then be determined as the following equation:

$$\frac{K_{ave}\,H_T\,W\,(P_{in}-P_{out})}{\mu L} = \sum_i \frac{K_i\,h_i\,W\,(P_{in}-P_{out})}{\mu L} \qquad \text{(A-12)}$$

For the same block dimensions, the fluid viscosity and the pressure boundary conditions for both fine and coarse scale blocks, the common terms can then be cancelled on both sides of the equation. The equation then becomes the following:

$$K_{ave}H_T = \sum_i K_i h_i \qquad \text{(A-13)}$$

The average (effective) permeability can then be obtained by rearranging the above equation as shown in Equation A-14.

$$K_{ave} = \frac{\sum_i K_i h_i}{H_T} \qquad \text{(A-14)}$$

Equation A-14: the derivation of effective permeability with arithmetic average on parallel bed

The above equation indicates that the average permeability is the height weighted arithmetic average of the individual layered permeability.

- Harmonic Upscaling Algorithm Derived Based on Serial Bed

The fluid flow in the series of beds can be illustrated with the following picture.
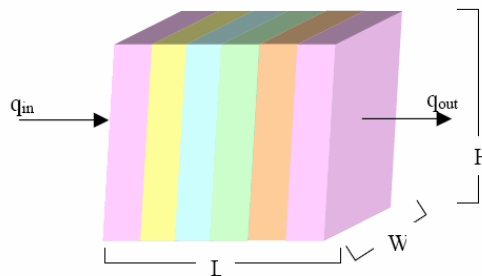
Fine Scale
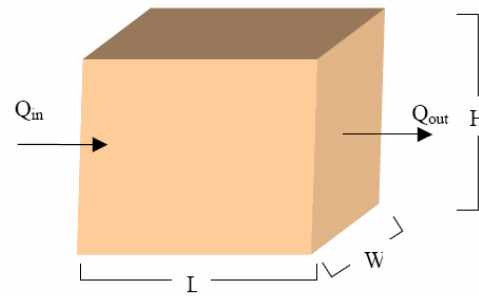
Coarse Scale

Figure A-4 Graphical representation of fluid flow in serial bed for harmonic upscaling algorithm derivation

With the law of mass conservation, the fluid flow into the block will be equal to the sum of the accumulation of the fluid flow within the blocks and the flow rate out from the block. Under the steady state at the equilibrium condition, the accumulation of fluid within the blocks will be negligible. Thus, the fluid will flow at the same flow rate across each bed. For the same flow rate across each bed, the pressure difference will then be proportional to the length of the bed, i. The fluid flow can be illustrated by applying Darcy's law of equation as the following equation:

$$\frac{K_{ave} H_T W (P_{in} - P_{out})}{\mu L} =$$

$$\frac{K_1 H_T W (P_{in} - P_{1,out})}{\mu L_1} + \frac{K_2 H_T W (P_{2,in} - P_{2,out})}{\mu L_2} + \ldots + \frac{K_n H_T W (P_{n,in} - P_{out})}{\mu L_n} \qquad \text{(A-15)}$$

For the same block dimensions and the fluid viscosity, the common terms can then be cancelled on both sides of the equation. The equation is then as follows:

$$\frac{K_{ave}(P_{in}-P_{out})}{L} =$$

$$\frac{K_1(P_{in}-P_{1,out})}{L_1} + \frac{K_2(P_{2,in}-P_{2,out})}{L_2} + \ldots + \frac{K_n(P_{n,in}-P_{out})}{L_n} \qquad (A-16)$$

From the equation above and the Darcy's fluid flow equation, the pressure differences between the blocks will serve as a function of the block permeability over the length i. Therefore, by assuming a proportion of pressure difference on each block over the total pressure differences with the ratio of block permeability over the length i, the average permeability can then be obtained as follows:

$$\frac{K_{ave}(P_{in}-P_{out})}{L} = \frac{K_1}{L_1}\frac{L_1}{K_1}\sum\frac{Ki}{Li}(P_{in}-P_{out}) + \frac{K_2}{L_2}\frac{L_2}{K_2}\sum\frac{Ki}{Li}(P_{in}-P_{out}) +$$

$$\ldots + \frac{K_n}{L_n}\frac{L_n}{K_n}\sum\frac{Ki}{Li}(P_{in}-P_{out}) \qquad (A-17)$$

Canceling some of the sum of the pressure difference and rearranging the above equation, the average permeability for the serial beds can be then obtained as the following equation:

$$K_{ave} = \frac{L}{\sum\limits_i L_i \big/ K_i} \qquad (A-18)$$

Equation (A-18): the derivation of effective permeability with harmonic average on serial bed.

The above equation indicates that average permeability on the serial bed can be defined with the length weighted harmonic average of each serial bed permeability.

Appendix B

The 10th SPE Comparative Solution Project

- ## Description of the 10th SPE Comparative Solution Project

This model has a sufficiently fine grid to make use of classical pseudoisation methods almost impossible. The model has a simple geometry, with no top structure or faults. The reason for this choice is to provide maximum flexibility in choice of upscaled grids.

At the fine geological model scale, the model is described on a regular Cartesian grid. The model dimensions are 1200 x 2200 x 170 (ft). The top 70 ft (35 layers) represents the Tarbert formation, and the bottom 100 ft (50 layers) represents Upper Ness. The fine scale cell size is 20 ft x 10 ft x 2 ft.

- ## Reservoir Description

The model consists of part of a Brent sequence. The model was originally generated for use in the PUNQ project. The top part of the model is a Tarbert formation, and is a representation of a prograding near shore environment. The lower part (Upper Ness) is fluvial.

Figure (B-1) shows the porosity for the whole model, and Figure (B-2) shows part of the Upper Ness sequence, with the channels clearly visible.

The fine scale model size is 60 x 220 x 85 cells (1.122x106 cells).
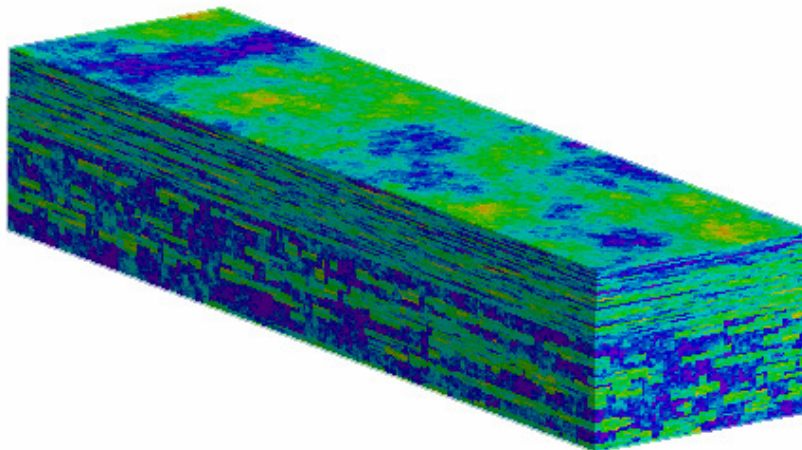
Figure B-1: Porosity for the whole model
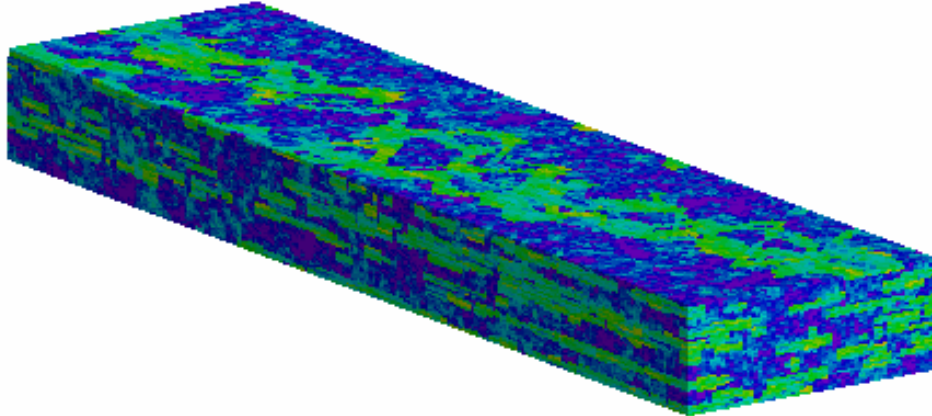
Figure B-2: Porosity for the Upper Ness sequence

Table B-1: Relative permeability and PVT data

Water properties	relative permeabilities
B_w = 1.01	
	krw(S) = (S*)2
c_w = 3.10^{-6} psi^{-1}	kro(S) = (1-S*)2
	S*= (S - Swc) / (1 - Swc - Sor)
viscosity 0.3 cp	Swc = Swi = 0.2
	Sor = 0.2
	krw(Sor) = kro(Swc) = 1.0

Table B-2: Dead oil PVT

(psi)	Bo	viscosity (cp)
300	1.05	2.85
800	1.02	2.99
8000	1.01	3

- **Initial Conditions**

Initial pressure: 6000 psi. at reference depth 12000 ft.

Surface densities: Oil 53 lb/ft^3 , water 64 lb/ ft^3.

Rock Compressibility: 10^{-6} psi^{-1}.

• Well Configuration

All wells vertical. All wells completed throughout formation.

Central Injector. Injection rate 5000 bbl/day (reservoir conditions). Max injection bottom hole pressure 10000 psi.

4 producers. Produce at 4000 psi bottom hole pressure.

Table B-3: Well Locations:

well name	X location, ft	Y location, ft
Injection Well I1	600	1100
Production Well P1	0	0
Production Well P2	1200	0
Production Well P3	1200	2200
Production Well P4	0	2200

• Tasks

Upscale the fine scale reservoir description to a suitable coarse grid. Any method of upscaling (single or multi-phase) can be used. Construct a coarse simulation model and simulate 2000 days of production.

- Report

To make fair comparisons between the different approaches, we need the following items to be reported:

Simulator used; impes or implicit; time step strategy (max dt, impes stability on or off, etc).

- Wells:

Injection Well: Bottom hole pressure.

Production Wells: Oil rate, water cut, cumulative oil production, water cut.

• **Downloadable Files**

Download relative permeability table. (.txt)

Download porosity and permeability file - por_perm_case2.zip (18.4MB) Corrected dataset - por_perm_case2a.zip (revised, 18.5MB)

File 1: Porosity (60 x 220 x 85)

File 2: Kx (i,j,k), i = 1-60, j = 1-220, k = 1,85

   Ky (i,j,k), i = 1,60, j = 1-220, k = 1,85

   Kz (i,j,k), i = 1,60, j = 1-220, k = 1,85

The SPE 10 model can be downloaded from this web- link:

http://www.spe.org/csp/datasets/set02.htm

Appendix C

Work Flow of the Model Preparation

- **Building the Model in Petrel^{TM}.**

    Basically the model looks like a block with the dimensions 1200 ft x 2200 ft x 170 ft; therefore two surface are created confining the Tarbert and Upper Ness formations, then a map is created to fit the model dimensions.

    - **Projection Systems:**

    Petrel does *NOT* utilize projection systems, but only works with UTM or Field units. All data to be used in a Petrel project will need to be converted to the same projection system outside of Petrel prior to data import. There is not an option to check for different projection systems either, so this is all user controlled and requires the user to check ALL the data imported into the project to make sure that (for example) the well positions are correct versus maps and/or other data.

    - **UNITS:**

    In addition, Petrel does not check which units the data imported is in. Petrel will allow for a mix of different units to be imported into the project, the typical example being well data and production data in feet, and maps and other data derived from seismic, in meters. The user must check to ensure that the data is imported with the correct units. It is *NOT* possible to convert units of data already imported into the project, but *data can be converted on import and export*.

    The best workflow to ensure common units in a Petrel project is:

    1. Check your data before import to decide which units are best to use as your project units. Petrel will allow you to use local coordinates, field, metric or a combination, which most commonly are UTM coordinates in XY-direction and feet in Z-direction.

2. When creating a new Petrel project, open the Project and select the units you want to use in your project. For the work of this thesis the data unit was set to be field unit.

3. For every object to be imported, check the file before import to see which units the data is listed in the file, and select unit conversion in the import dialogue if needed.

4. If you see that a data object is unit inconsistent with the other data in the project, delete it and re-import it with the correct conversion.

In the process window, choosing make simple grid is the start to describe the model geometry and location, giving a name to the model is done in this window, the thickness of the reservoir is 170 ft start at depth 12000 ft. In the make simple grid window the values (-12000) and (-12170) is assigned in top limit and bottom limit respectively.

The geometry of the model in horizontal direction was specified as minimum and maximum values.

X minimum : 0   X max : 1200

Y minimum : 0   Y max : 2200

The grid increment is the dimension of the cell which is defined as 'node', and it was set to be 20 and 10 for both directions X and Y respectively. Clicking on OK then the model has been created.

Node = the dimension in one direction (ft)/ Number of cell in the same one direction

- **Creating the Structure Framework**

If the process is run without using surfaces to define horizons, the result is a skeleton grid. A 'skeleton grid' is a Petrel term for the framework that is made as the first step towards defining a 3D grid. A 'skeleton grid' consists of a Top, mid, and bottom mesh defined by 'pillars'. The pillars define the lateral position of the corners in the three meshes, and the z-position is defined as the bottom, mid point, and the top of

the pillars. After such a 'skeleton grid' is generated, it needs to be further subdivided in the vertical direction. This is done by inserting surfaces. The topmost and the bottommost surface that are inserted define the top and the bottom of the final 3D grid. Hence, the top and the bottom 'skeleton grid' is usually outside the final 3D grid.

The reason why 3D grids are generated this way in Petrel is that the gridding process starts with modelling the faults which are defined using pillars. Those pillars are then used to define the geometry of the 3D grid. The processes used to make grids based on fault modelling are 'Fault Modelling' and 'Pillar Gridding'.

We need to have real grid not the skeleton to build out properties in it so this model should be converted to real grid , and that can be done by convert to surface, and this now the input to the horizon and layers.

- **Making Horizon:**

And now "Horizon" should be created. This process usually defines the main depositional units of the 3D grid and are, in most cases, the layers identified and interpreted on seismic data. Make Horizon samples input surfaces into the 3D Grid. The input can be mapped surfaces from seismic or well tops, line interpretations from seismic, or any other point or line data defining the surface. Note that a 'Horizon' in Petrel is a surface that is a part of the 3D grid.

- **Making Zone:**

Zones are defined as the interval between to horizons. This process defines the sub-units of the 3D grid and is usually the zone division defined by interpreted formation markers from the wells (Well Tops). Make Zones inserts additional horizons (and zones) into the 3D Grid by inserting isochores up or down from the previously input horizons. The isochores can be gridded thickness maps or calculated directly from well tops. Zones can also be defined as specific thickness intervals or percentages of the main zone.

- **Layering:**

The final step is to make the final vertical resolution of the 3D grid, in this case (SPE 10) was assigned as 85 layers.

• Importing Grid Properties and Upscaling

Once the geometrical model is created, it is possible to assign the properties and that can be done be starting with the fine model. The grid property data provided with the 10th SPE example comprises the porosity and the permeability in two files, these files are just data with no key words but it is in Eclipse format, therefore one must add the necessary key words BOX PORO ENDBOX to the porosity data file, and BOX PERMX / PERMY / PERMZ ENDBOX in the permeability file. Now these data files can be loaded into the model.

Entering the explorer window and then clicking on properties, and by right click chose from the dialog 'import on selection'.

The format of the imported data should be (Eclipse keyword (grid properties) (*.DATA)). By inserting the SPE 10 data file the Petrel[TM] will start assigning the properties inside the geometrical model. And under a file called 'convert' in the explorer window the properties will be found (PERMZ, PERMX, PERMY, PORO).

For upscaling, in the menu bar inter file and click on 'Reference Project tool'. In the reference project tool you will find two projects, the left hand side is the project you want to construct (coarse), and the right hand side is the fine model or the reference model that you would take the properties from it.

On the upper right corner you will find the icon (open project), click on it to insert or include the fine model.

In the process window open 'Upscaling', and in this thesis the geometry was decided at the beginning of the work, so properties is been chosen for upscaling. Two methods of upscaling for the properties for each model were chosen which analytical methods are and the numerical method, upscaling in the petrel[TM] takes about 10 to 20 minutes for each model.

- **Exporting the Model to Eclipse**

  After the model setup is finished, it can be exported. The output format needed for the dynamic simulation (Eclipse in our case) is *.GREDECL for the grid geometry and for the grid properties as well.

  - **Creating the Schedule Section**

  The basic steps to create the schedule file are described. First set the unit to Field, and import the grid data, properties, well events, and well trajectories. Add to group of wells and name them inj and prod and introduce well I1 to the inj group and the producing wells P1, P2, P3 and P4 to the prod group, then select well by well and set PERFORATIONS, INJ/PRODCONTROL, COMPDATA, WELSPECS. For the injection well set the Control Mode to 'Rate' in 'Reservoir Condition' at 5000 bbl/day, and the 'BHP Limit' to 10000 psi, whereas for the producers set the Control Mode to 'BHP' and set the value to 4000 psi then from the 'Setup' menu select 'Time Frame Work' and set time steps.

  - **Creating the Data File for the Eclipse Simulator**

  The data file is short and simple. Short because the grid, properties, and schedule files are included, and simple because only one rock region and one PVT region exists, and the fluid are water and dead oil, with no aquifer and no special features for an example faults. A copy of the data file is shown below for model 2 (30*55*85).

```
--------------------------- Runspec Section ---------------------------------
NOECHO
RUNSPEC
TITLE
 SPE10 example 30X55X85=140,250


DIMENS
-- NX   NY   NZ
  30   55    85  /


-- Phases present


OIL


WATER


--GAS


--DISGAS


-- Units


FIELD


TABDIMS


-- NoSatTabl    MaxNodesSatTab  MaxFIPReg      MaxSatEndpointsDepthTab
--      NoPVTTab      MaxPressNodes    MaxRsRvNodes
    1     1    20    20    1    20    1   /


-- Well dimension
WELLDIMS
-- MaxNo  MaxPerf  MaxGroup MaxWell/Group
```

```
   5    85    2    4 /


START
  1 'JAN' 1990 /


-- Defining aquifer dimensions for all aquifers


--UNIFOUT


--NOSIM


NSTACK
 10 /



MESSAGES
8* 10000 500 100 1* /


------------------------------ Grid Section ----------------------------------


GRID


GRIDFILE
2 /


-- Including the indiviual grid file


INCLUDE
 'model 4 GP.GRDECL' /


INIT


--NNC
```

```
--/


--NEWTRAN


----------------------------- Edit Section ----------------------------------


----------------------------- Properties Section -----------------------------


PROPS


ROCK
-- RefPressure      Compressibility
-- for PoreVol Calc
--PSIA            1/PSIA
 6000             1.0E-06 /


SWOF
--Sw   Krw   Krow   Pcwo
 0.2    0.0000 1.0000 0
 0.25   0.0069 0.8403 0
 0.3    0.0278 0.6944 0
 0.35   0.0625 0.5625 0
 0.4    0.1111 0.4444 0
 0.45   0.1736 0.3403 0
 0.5    0.2500 0.2500 0
 0.55   0.3403 0.1736 0
 0.6    0.4444 0.1111 0
 0.65   0.5625 0.0625 0
 0.7    0.6944 0.0278 0
 0.75   0.8403 0.0069 0
 0.8    1.0000 0.0000 0
 1      1.0000 0.0000 0 /
```

```
PVDO
-- Pressure    Bo     Vo
   300      1.05   2.85
   800      1.02   2.99
   8000     1.01    3.00 /


PVTW
--Depth Bw    Comp  Vw   Cv
 12000  1.01 3.0E-6  0.3   0.0
 /


DENSITY
-- Oil   Water   Gas
  53    64    0.0702 /


----------------------------- Regions Section -------------------------------


----------------------------- Solution Section ------------------------------


SOLUTION


-- Equilibrium data


EQUIL


-- DATUM   DATUM   OWC    OWC    GOC    GOC    RSVD   RVVD
ACCURACY OPT
-- DEPTH  PRESS  DEPTH  PCOW  DEPTH   PCOG   TABLE TABLE No of
LAYERS
 12000.000 6000.00   12170    0     0     0     0 /


RPTSOL
-- SOIL
```

```
-- SWAT
-- SGAS
-- PRESSURE
 RESTART /


------------------------------ Summary Section ------------------------------


SUMMARY


----------------------------------------------
--Output of production data/pressure  for FIELD:
----------------------------------------------
FOPR


FOPT


FPR


FWCT
-----------------------------------------
--Output of production data for all wells:
-----------------------------------------
WOPR
'P1'  'P2' 'P3' 'P4'  /


WBHP
'I1' 'P1' 'P2' 'P3' 'P4' /


WOPT
'P1'  'P2' 'P3' 'P4'  /


WWCT
'P1' 'P2' 'P3' 'P4'  /
```

RPTONLY

RUNSUM

SEPARATE

RPTSMRY
 1 /

DATE

LOTUS

TCPU
----------------------------- Schedule Section -------------------------------

SCHEDULE

INCLUDE
 'model 4 30X55X85.SCH' /

END

A copy of the Schedule file is shown below for model 2 (30*55*85).

```
ECHO
-- CONTROLS ON OUTPUT AT EACH REPORT TIME
--
RPTRST
  3 1 1 0 0  3 0 0 0 0  0 0 0 0 0  0 3 6 1 0 /
--
RPTSCHED
  0 0 0 0 0  0 0 2 2 0 /


NOECHO


WELSPECS
    'I1'    'inj'  15  28  12000.000    'WATER' 7* /
    'P1'    'prod'  1   1  12000.000     'OIL' 7* /
    'P2'    'prod'  30   1  12000.000     'OIL' 7* /
    'P3'    'prod'  30  55  12000.000      'OIL' 7* /
    'P4'    'prod'   1  55  12000.000      'OIL' 7* /
/


COMPDAT
-- WELL      I   J   K1  K2        Sat.    CF     DIAM      KH SKIN ND
DIR   Ro
    'I1' 2*   1  85    'OPEN' 2*    0.850 3*       'Z' 1* /
    'P1' 2*   1  85    'OPEN' 2*    0.850 3*       'Z' 1* /
    'P2' 2*   1  85    'OPEN' 2*    0.850 3*       'Z' 1* /
    'P3' 2*   1  85    'OPEN' 2*    0.850 3*       'Z' 1* /
    'P4' 2*   1  85    'OPEN' 2*    0.850 3*       'Z' 1* /
/


GRUPTREE
```

```
 'INJ'     'FIELD'  /
 'PROD'     'FIELD'  /
/


WCONPROD
    'P1'     'OPEN'     'BHP' 5*   4000.000  8* /
    'P2'     'OPEN'     'BHP' 5*   4000.000  8* /
    'P3'     'OPEN'     'BHP' 5*   4000.000  8* /
    'P4'     'OPEN'     'BHP' 5*   4000.000  8* /
/


WCONINJE
    'I1'     'WATER'     'OPEN'     'RESV'  1*  5000.000  10000.000  3* /
/


-- 1.000000 days from start of simulation ( 1 'JAN' 1990 )
DATES
 2 'JAN' 1990 /
/


-- 120.000000 days from start of simulation ( 1 'JAN' 1990 )
DATES
 1 'MAY' 1990 /
/


-- 243.000000 days from start of simulation ( 1 'JAN' 1990 )
DATES
 1 'SEP' 1990 /
/


-- 365.000000 days from start of simulation ( 1 'JAN' 1990 )
DATES
 1 'JAN' 1991 /
```

```
/


-- 485.000000 days from start of simulation ( 1 'JAN' 1990 )

DATES

 1 'MAY' 1991 /

/

-- 608.000000 days from start of simulation ( 1 'JAN' 1990 )

DATES

 1 'SEP' 1991 /

/

-- 730.000000 days from start of simulation ( 1 'JAN' 1990 )

DATES

 1 'JAN' 1992 /

/

-- 851.000000 days from start of simulation ( 1 'JAN' 1990 )

DATES

 1 'MAY' 1992 /

/


-- 974.000000 days from start of simulation ( 1 'JAN' 1990 )

DATES

 1 'SEP' 1992 /

/


-- 1096.000000 days from start of simulation ( 1 'JAN' 1990 )

DATES

 1 'JAN' 1993 /

/

-- 1216.000000 days from start of simulation ( 1 'JAN' 1990 )

DATES

 1 'MAY' 1993 /

/

-- 1339.000000 days from start of simulation ( 1 'JAN' 1990 )
```

```
DATES
 1 'SEP' 1993 /
/
-- 1461.000000 days from start of simulation ( 1 'JAN' 1990 )
DATES
 1 'JAN' 1994 /
/


-- 1581.000000 days from start of simulation ( 1 'JAN' 1990 )
DATES
 1 'MAY' 1994 /
/


-- 1704.000000 days from start of simulation ( 1 'JAN' 1990 )
DATES
 1 'SEP' 1994 /
/


-- 1826.000000 days from start of simulation ( 1 'JAN' 1990 )
DATES
 1 'JAN' 1995 /
/


-- 1946.000000 days from start of simulation ( 1 'JAN' 1990 )
DATES
 1 'MAY' 1995 /
/
```

```
DATES
 1 'JUL' 1995 /
/
-- END OF SIMULATION
```

NOMENCLATURE

K   absolute permeability in fine cell

K   effective absolute permeability in coarse cell

K   vertical perm

K   horizontal perm

Q   the flow rate

A   cross sectional area

P   pressure

Pc   capillary pressure

X   length in x direction

μ   viscosity

h   reservoir thickness

L   reservoir length

Φ   porosity

$\Delta P/\Delta L$ pressure change across reservoir length

g   gravitational force

PV   pore volume

Vbulk   bulk volume (grid block volume)

Subscript

n   number of blocks in one direction

i,j,k   block index

x,y,z   directional indication (x,y,z direction)

A   arithmetic average

G	geometric average
H	harmonic average
ω	Power factor
Fine	properties of fine scale
Coarse	properties of coarse scale